AFRL-RV-HA-TR-2007-1202

An Evaluation of Cirrus Cloud Forecasts from Three Operational Weather Prediction Models

Donald C. Norquist

10 October 2007

AIR FORCE RESEARCH LABORATORY
Space Vehicles Directorate
29 Randolph Rd
AIR FORCE MATERIAL COMMAND
Hanscom AFB, MA 01731-3010

AFRL-RV-HA-TR-2007-1202

This technical report has been reviewed and is approved for publication.

/signed/
Lt. Col. Bruce P. Anderson, Deputy Chief
Battlespace Environment Division

/signed/
Donald C. Norquist
Battlespace Surveillance Innovation Center

/signed/
Major Brian D. Griffith, Chief
Battlespace Surveillance Innovation Center

REPORT DOCUMENTATION PAGE

Form Approved
OMB No. 0704-01-0188

PLEASE DO NOT RETURN YOUR FORM TO THE ABOVE ADDRESS.

1. REPORT DATE *(DD-MM-YYYY)*	2. REPORT TYPE	3. DATES COVERED *(From - To)*
31-10-2007	Scientific, Interim	

4. TITLE AND SUBTITLE

An Evaluation of Cirrus Cloud Forecasts from Three Operational Weather Prediction Models

5a. CONTRACT NUMBER

5b. GRANT NUMBER

5c. PROGRAM ELEMENT NUMBER
621010F

6. AUTHORS

Donald C. Norquist

5d. PROJECT NUMBER
1010

5e. TASK NUMBER
0T

5f. WORK UNIT NUMBER
A1

7. PERFORMING ORGANIZATION NAME(S) AND ADDRESS(ES)

Air Force Research Laboratory / RVBYA
29 Randolph Road
Hanscom AFB, MA 01731-3010

8. PERFORMING ORGANIZATION REPORT NUMBER
AFRL-RV-HA-TR-2007-1202

9. SPONSORING/MONITORING AGENCY NAME(S) AND ADDRESS(ES)

10. SPONSOR/MONITOR'S ACRONYM(S)

11. SPONSOR/MONITOR'S REPORT NUMBER(S)

12. DISTRIBUTION/AVAILABILITY STATEMENT

Approved for public release; distribution unlimited

13. SUPPLEMENTARY NOTES

14. ABSTRACT

Cirrus clouds are known to impact certain Air Force missions and systems. Mission planners need accurate cirrus predictions in advance of system deployment. This report describes a project to evaluate the ability of operational mesoscale numerical weather prediction models to predict cirrus cloud characteristics. The Air Force Weather Agency (AFWA) MM5 and the National Centers for Environmental Prediction (NCEP) North American Mesoscale (NAM) prognostic models, along with the AFWA Diagnostic Cloud Forecast (DCF) diagnostic algorithm, were considered in the study. Geostationary Operational Environmental Satellite (GOES) imagery channel data were processed to detect ice cloud picture elements (pixels) and to retrieve cloud top height and ice water path as a reference. The presence/absence of cloud ice in the model grid cell was compared with the presence of ice cloud in within-grid-cell pixels. Results showed that the comparison statistics vary significantly by region and to a lesser degree by season. Study results have been summarized for use in providing guidance supporting high altitude laser system tests.

15. SUBJECT TERMS

Cirrus clouds, satellite imagery, mesoscale weather models, ice water path, cloud top height

16. SECURITY CLASSIFICATION OF:			17. LIMITATION OF ABSTRACT	18. NUMBER OF PAGES	19a. NAME OF RESPONSIBLE PERSON
a. REPORT	b. ABSTRACT	c. THIS PAGE			Donald C. Norquist
U	U	U	SAR	61	19B. TELEPHONE NUMBER *(Include area code)*

Contents

Illustrations

Tables

Acknowledgements

The author thanks Dan DeBenedictis for file server and network support that ensured access to AFWA, NCEP and Naval Research Laboratory data sources. Thanks are also given to Doug Hahn for his tireless care of the AFRL Environmental Satellite Data Facility, the source of the GOES-12 imagery data. Joe Turk is his counterpart in staging the GOES-11 data from the NRL ground station, whose efforts are also gratefully appreciated. Brad Ferrier at NCEP provided guidance on the use of the NAM forecast data. Diagnostic cloud forecast data was supplied by the Weather Data Analysis Capabilities data provider process at AFWA. Finally, funding support for this project was provided in part by Major Steve Cocks of the Missile Defense Agency.

1 INTRODUCTION

Cirrus clouds have been shown to have an impact on certain Air Force missions and systems. Some examples are high altitude reconnaissance and laser propagation for communications and missile defense. Koenig et al. (1993) analyzed the potential impact of cirrus on laser propagation by modeling the transmission through cirrus properties assumed for distinct altitude layers. Cirrus extinction was derived based on the assumption of spherical ice particles. They found that the laser power loss in long path lengths depended on the assumed cirrus extinction when the laser is directed nearly horizontally. Norquist et al. (2008) executed laser transmission models in slant paths using cirrus cloud properties as retrieved from observations. Their results showed that the laser beam can experience significant attenuation in long paths through the cirrus when the source and receiver are close in altitude but separated by distances of 30 km or more horizontally. Therefore, accurate predictions of cirrus clouds are needed for laser system mission planning in advance of their deployment.

Having characterized the effects of cirrus on laser propagation in the earlier study, it is necessary to document the accuracy of cirrus predictions by current weather prediction systems. Norquist et al. (2008) state that since any visible cirrus clouds are likely to have an appreciable impact on laser propagation, their macrophysical properties (location, altitude, coverage) are probably more important for mission planning than their microphysical properties. Thus, the current study focuses on the ability of mesoscale weather prediction (MWP) models to predict the spatial and temporal characteristics of cirrus over a region of interest. In particular, emphasis is placed on determining area of coverage by cirrus and the reliability of MWP models to

correctly predict which portions of the region will be covered. Altitude and ice water mass of the cirrus are considered but are of secondary importance in this project.

Some recent studies have been conducted to evaluate the ability of MWP models to predict ice clouds. Chiriaco et al. (2006) compared the predictions by several microphysical schemes in the fifth-generation Pennsylvania State University-National Center for Atmospheric Research (PSU-NCAR) Mesoscale Model (MM5; Dudhia 1993) with active and passive remote sensors at a single location over long time periods. Their focus was on the microphysical and optical properties of the clouds, and they found that the best scheme simulated cirrus at the site in about 2/3 of the selected cirrus events. Lewis (2006) looked at two cirrus episodes in the southwestern United States as simulated by the MM5 as executed operationally at the Air Force Weather Agency (AFWA). A subjective assessment of the mass, motion and moisture fields of the model predictions showed that the dynamical and hydrological processes necessary for cirrus formation were present, but that for the two cases studied they produced less cirrus in area covered than was detected from satellite imagery.

The goal of this project was to comprehensively assess the cirrus prediction performance of the AFWA MM5 and the National Center for Environmental Prediction (NCEP) North American Mesoscale (NAM) models. Diagnoses of cirrus clouds from the AFWA Diagnostic Cloud Forecast (DCF) algorithm (AFWA, 2007a) applied as a post processor to AFWA MM5 forecasts were also evaluated. The three forecast methods were assessed over approximately 30-day periods in each season over two different climatic regions. Satellite imagery was used as a reference for these evaluations to allow assessments of the models' ability to predict cirrus on horizontal scales of 100s of

km. This assessment will provide information on the use of these forecasts to support Department of Defense system tests in the near future.

In this paper, results of comparing MM5 and NAM model predictions and DCF algorithm forecasts of ice cloud with satellite depictions are presented for periods in Winter, Spring and Summer 2007 over two regions in North America: the northeast United States (NEUS) region (40-47 N latitude, 70-81 W longitude) and the southwest United States (SWUS) region (30-40 N latitude, 105-122 W longitude). Fall 2006 MM5 and NAM predictions were also assessed. Twice-daily 24- and 36-hour forecasts were compared with ice cloud masks, ice water path and cirrus top height as retrieved from the Geostationary Operational Environmental Satellite – 12 (GOES-12) imagery for the NEUS region and GOES-11 imagery for the SWUS region. Statistics based on objective comparisons of the gridded representations of model and algorithm forecasts and GOES analyses are reported for the two seasonal periods in both regions. Some preliminary conclusions are reached about the characteristics of the cirrus predictions of the models/algorithms based on this study.

2 DATA

AFWA executes the MM5 over North America on a grid of 45 km grid spacing with a nested window over the continental United States (CONUS) of 15 km grid spacing. Both nests are discretized vertically into 41 model layers with a model top at 50 hPa. Physical parameterizations relevant to cirrus formation utilized in the AFWA MM5 are the moist convective scheme of Kain and Fritsch (1990) and the explicit microphysics formulation of Reisner et al. (1998). The model is executed at 06 and 18 UTC each day out to 72 hours (45 km grid) and 48 hours (15 km grid).

AFWA MM5 06 and 18 UTC 15 km grid forecasts of 21, 24, 33 and 36 hours were obtained each day for the periods 1 November - 2 December 2006 (Fall), 13 February – 14 March 2007 (Winter), 8 May – 6 June 2007 (Spring) and 1 – 30 August 2007 (Summer). Pressure, temperature, height, humidity and ice water mixing ratio (≥ 0.001 g/kg) on model layers were extracted for the NEUS and SWUS regions. These data represented the MM5 forecasts in the comparisons conducted in this project.

NCEP executes the Weather Research and Forecasting (WRF) system with the Nonhydrostatic Mesoscale Model (NMM) core, which is referred to as the WRF-NMM (NCEP, 2007). NCEP currently utilizes this forecasting system as their North American Mesoscale (NAM) weather prediction model. Forecasts of 12 km grid spacing are executed from 00, 06 12 and 18 UTC daily. NCEP interpolates the forecast fields to a Lambert Conformal grid of 32.46 km grid spacing covering North America and surrounding ocean areas, on constant pressure levels of 25 hPa intervals to 50 hPa, then 30, 20 and 10 hPa levels. The current operational NAM uses the Janjic (1994) moist convective scheme and the Ferrier et al. (2002) explicit cloud microphysics algorithm.

NAM 06 and 18 UTC forecasts of 21, 24, 33 and 36 hours duration on the 32.46 km grid were obtained each day for the same time periods as mentioned above in the AFWA MM5 data description. Gridded temperature, height, humidity and ice water mixing ratio (≥ 0.001 g/kg) on constant pressure levels were extracted for the NEUS and SWUS regions. These data constituted the NAM forecasts utilized in the comparisons for this report.

AFWA's DCF algorithm is executed as a postprocessor to the MM5 model and

the World-wide Merged Cloud Analysis (WWMCA, AFWA, 2007b). Ten days of twice-daily MM5 forecasts are paired with forecast valid time WWMCA gridded analyses to generate statistical relationships between selected MM5 predictor variables and the WWMCA cloud properties (cloud cover, top and base altitude and type) for as many as four cloud layers. The relationships are then applied to ensuing MM5 forecasts to diagnose cloud layer properties at prediction times.

AFWA DCF 06 and 18 UTC forecasts of 21, 24, 33 and 36 hours on the CONUS grid of 15 km spacing were acquired each day for the time periods mentioned above. Cloud cover (aka amount), cloud top height, cloud base height and cloud type for up to three layers of clouds were extracted for the NEUS and SWUS regions. Only cloud properties for diagnosed clouds (cloud cover diagnosed to be greater than 0%) are included in the data. Zero values indicate the absence of clouds in some or all of data fields corresponding to the three cloud layers.

GOES-11 imagery channels of 0.65, 3.7, 6.7 10.8 and 12 μm on picture elements (pixels) of approximately 5 km on a side were obtained from the Naval Research Laboratory in Monterey, CA. Image files containing data for western North America and the eastern Pacific Ocean were obtained for image times of 06 and 18 UTC (or if missing, the nearest available image times prior to but within three hours of these times). Imagery data were extracted for the SWUS region. GOES-12 imagery files created by the Air Force Research Laboratory GOES-12 ground station at image times nearest but before 06 and 18 UTC contained data for eastern North America and the western Atlantic. GOES-12 imagery channels of 0.65, 3.7, 6.7 10.8 and 13 μm on approximately 5 km pixels were extracted for the NEUS region. The GOES-11 and

GOES-12 imagery data served as the basis for comparison with MM5, NAM and DCF ice cloud predictions in the NEUS and SWUS regions.

3 METHOD

Each regional GOES image file was processed to conduct cloud detection, cloud phase discrimination and cloud property retrieval. The cloud detection and property retrieval algorithm of Gustafson and d'Entremont (2000) was utilized to distinguish between clear, liquid cloud and ice cloud pixels, and for the ice pixels it retrieved estimates of (among other properties) ice water path (IWP), cloud top height (CTH) and visible optical depth. AFWA MM5 forecast height and temperature profiles on the 15 km grid were used to convert retrievals of cloud top temperature to CTH. Norquist et al. (2008) compared GOES-12 ice cloud retrievals from this algorithm with radar and lidar measurements of CTH and radar/lidar retrievals of IWP for a series of cirrus events at Hanscom Air Force Base, MA in 2005. They found that the GOES-12 CTH estimates were on average about 1.1 km lower in altitude than the radar/lidar measurements. They also found that GOES-12 IWP retrievals were on average smaller than the radar/lidar retrievals by a factor of 3 to 4. Cloud detection is considered the strongest feature of the algorithm, and cloud phase discrimination is also thought to be reliable. It should be emphasized, however, that Norquist et al. (2008) found that the GOES ice cloud detection failed to detect cirrus with visible optical depths of less than 0.5 as determined from the radar/lidar retrievals. Therefore, the cirrus detected by the GOES algorithm are likely limited to an optical depth of about 0.5 and greater and might not account for optically thinner cirrus. This may result in a slight under representation of the total cirrus coverage, especially near the cloud edges.

The first step in the forecast model – GOES comparison processing was to identify the GOES pixels associated with (lying closest to) each MM5, NAM or DCF grid point. These pixels can be thought of as lying within the corresponding model/algorithm grid cell. For the 15 km MM5 and DCF grids, on average 9 pixels were within each cell, while for the 32.5 km NAM grid, about 40 pixels on average were within each cell. This needed to be done just once for each combination of region and forecast model.

MM5 and NAM forecast fields of temperature, height, humidity and ice water mixing ratio (and for MM5, pressure) were used in the processing to compare ice cloud predictions with satellite imagery. In each model grid cell, the tropopause is computed from the pressure, temperature and height profile using the algorithm of Roe and Jasperson (1980). Vertical profiles of predicted pressure (for MM5 only), temperature, height, humidity and ice water content (converted from ice water mixing ratio by multiplying by air density), and the computed tropopause, were interpolated in time (if necessary) between the 21 and 24 or 33 and 36 hour forecast times, to the time of the comparative GOES image. For the time-interpolated MM5 profiles, the height at the top of each model layer was computed. The average height between constant pressure levels was used as the height at the top of each "pressure layer" for NAM. Next, the model layers (or pressure layers for NAM) with non-zero ice water content were identified, and were numerically integrated (each multiplied by layer depth and summed) to compute the IWP, and the height of the top of the topmost ice cloud layer was set as the CTH. Only model grid cells with CTH $\geq$ 6 km were considered in the comparison with GOES. Such a grid cell was counted as a model ice grid point and it's computed IWP and CTH were stored.

In the DCF processing, three layers of the following four forecast quantities were used from the pair of forecast times bracketing the imagery time: cloud cover, cloud type, cloud base altitude and cloud top altitude. It also used all of the MM5 model levels of pressure, temperature and height from the two corresponding MM5 files, as well as the MM5 grid point terrain height values. The MM5 quantities were used to compute the tropopause height following the method of Roe and Jasperson (1980) for each regional grid point for the two MM5 times. The MM5 grid point lying closest to each DCF grid point provided the tropopause height for use in the DCF processing. The algorithm then processed each within-region DCF grid point in turn. The algorithm considered each of the three layers of the time-pairs of cloud cover, type, base and top values. For each of the two forecast times, it identified (if any) the highest (in altitude) of the three cloud layers with non-zero cloud cover and with a cirrus type (types 8 or 9) that had a top height ≥ 6 km. If only one of the two forecast times had such a layer, the cover was time interpolated (to the imagery time) using a zero value at the appropriate forecast time. The nonzero forecast time's top height was assigned as the interpolated top height. If both forecast times have such a layer, a linear interpolation in time to the imagery time was used for both the cover and top height. The nearest neighbor MM5 tropopause heights were also interpolated in time to the imagery time. At this point the processing of interpolated DCF cirrus cover, top height and MM5 tropopause height proceeded in a manner analogous to that for the MM5 and NAM cirrus ice water path, top height and tropopause height grid values.

GOES ice pixels within the model/algorithm grid cell with a CTH ≥ 6 km (if any) were counted, and for a non-zero count the retrieved IWP and CTH were averaged. The

fraction of ice pixels within the grid cell represented the percent GOES cirrus cover. If the within-cell ice pixel count was at least one, then the collective within-cell ice pixels were considered as a GOES ice grid point and the averaged IWP and CTH, along with the cover, were stored. If both model/algorithm and GOES were ice grid points, then the fcst Y / GOES Y counter was incremented for that grid cell and the respective IWP (cover for DCF) and CTH values were paired for comparison. If either or both model or GOES were not ice grid points, then the corresponding category (fcst Y / GOES N, fcst N / GOES Y, fcst N / GOES N) was incremented.

There are two reasons why a single GOES pixel is considered sufficient to identify the model grid point as an ice grid cell for the purposes of satellite detection. First, as previously mentioned the GOES ice cloud detection is limited to visible optical depths of about 0.5 and higher. The presence of any detected ice pixels in a grid suggests the likelihood of undetected ice pixels nearby. Second, it is important to account for the presence of any cirrus in evaluating the predictive models/algorithm. Because of the need to avoid cirrus in certain operations, it is important that the prediction systems anticipate any cirrus occurrence in a region of interest.

Once all model/algorithm grid cells were processed for an individual forecast time (24-h or 36-h), the total number of all model/algorithm ice grid points, the total number of all GOES ice pixels, and the count of the four ice grid point Y/N categories were recorded, along with the IWC, cover and CTH pairs and tropopause height for the Y/Y ice grid points. Then after processing of all forecasts for both 24-h and 36-h durations was completed for the seasonal period, a totaling of the individual forecast totals and their percentages of the total number of grid points (for total model/algorithm ice grid

points and Y/N category counts) and total number of GOES pixels was computed. Individual forecast averages and overall period averages of the models/algorithm and GOES IWP, cover and CTH was computed for all Y/Y ice grid points. In addition, all such CTH values were compared to the tropopause heights for each grid point, and if it exceeded the trop height it was adjusted to the trop height. Then a subsequent CTH average was computed over all Y/Y ice grid points for the models, algorithm and GOES, which is referred to as the trop adjusted CTH averages. Finally a count and percentage of the Y/Y grid points whose CTH was so adjusted were computed.

4 RESULTS

Regional cirrus coverage and location of cirrus within the region are the primary metrics of interest in the current prediction evaluation. The assessment of the model/algorithm forecasts begins with their performance on the regional scale, and then investigates the placement of predicted cirrus within the regions. First, examples of selected forecasts are illustrated as forecast maps and compared with maps of detected cirrus. Next, summary statistics of the 24- and 36-hour ice cloud forecasts and GOES ice cloud detection over the four seasonal periods are compared. This is followed by a review of the fcst/GOES Y/N category totals over each seasonal period, an indicator of overall forecast skill. Indices drawn from the Y/N statistics are discussed. Finally, the predicted and retrieved ice water path, cover and cirrus top height at the fcst Y / GOES Y grid cells are compared.

4.1 Selected Map Comparisons

Cirrus forecast maps from the MM5 and NAM models and the DCF algorithm are shown in Figures 1-19 in comparison with maps of retrieved GOES cirrus properties.

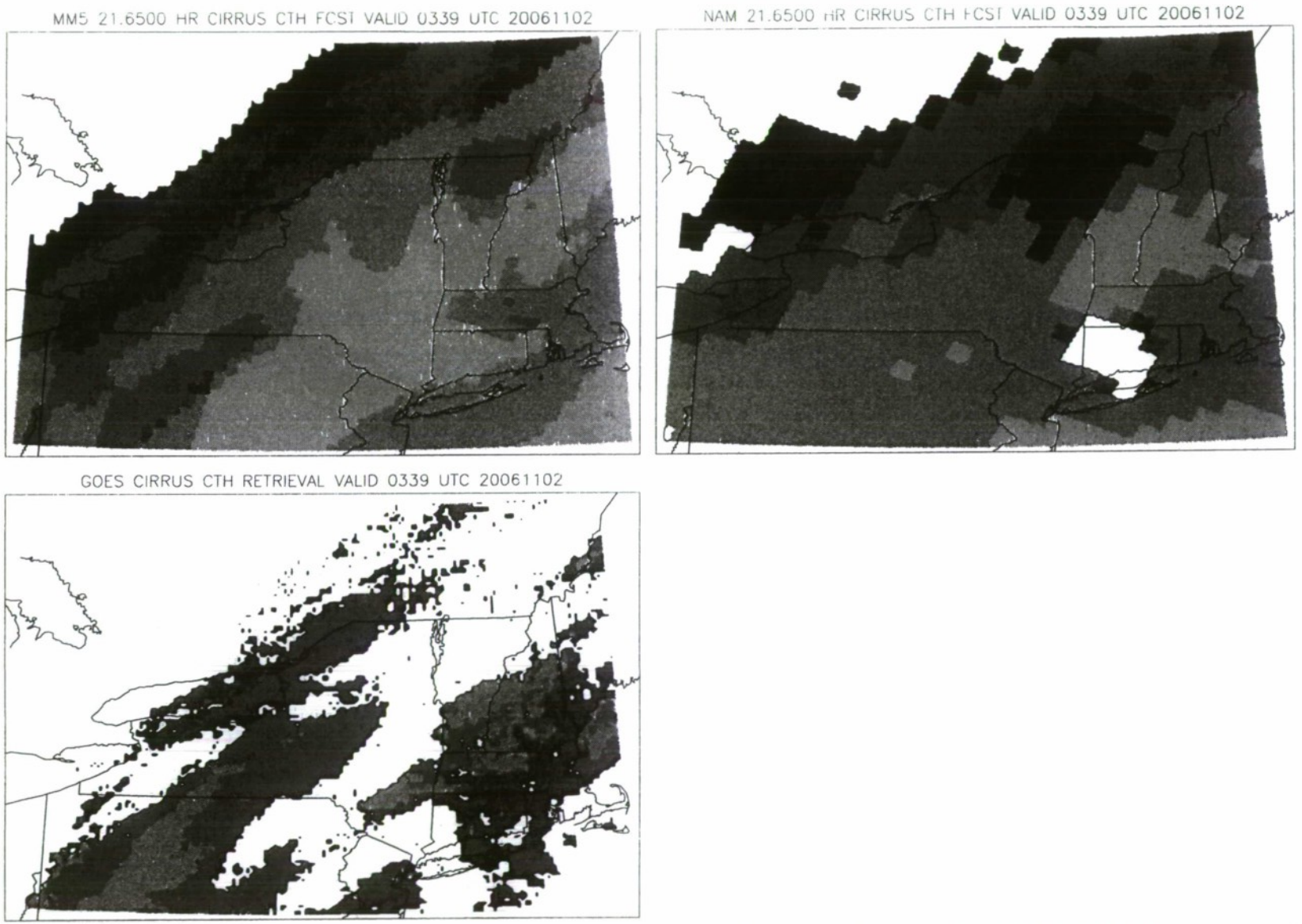

Figure 1. NEUS cirrus top height (km) valid at 0339 UTC 2 November 2006 from 21.65-h MM5, NAM forecasts and GOES-12 analysis. Gray scales intervals are 1 km starting with black shading at 6 km.

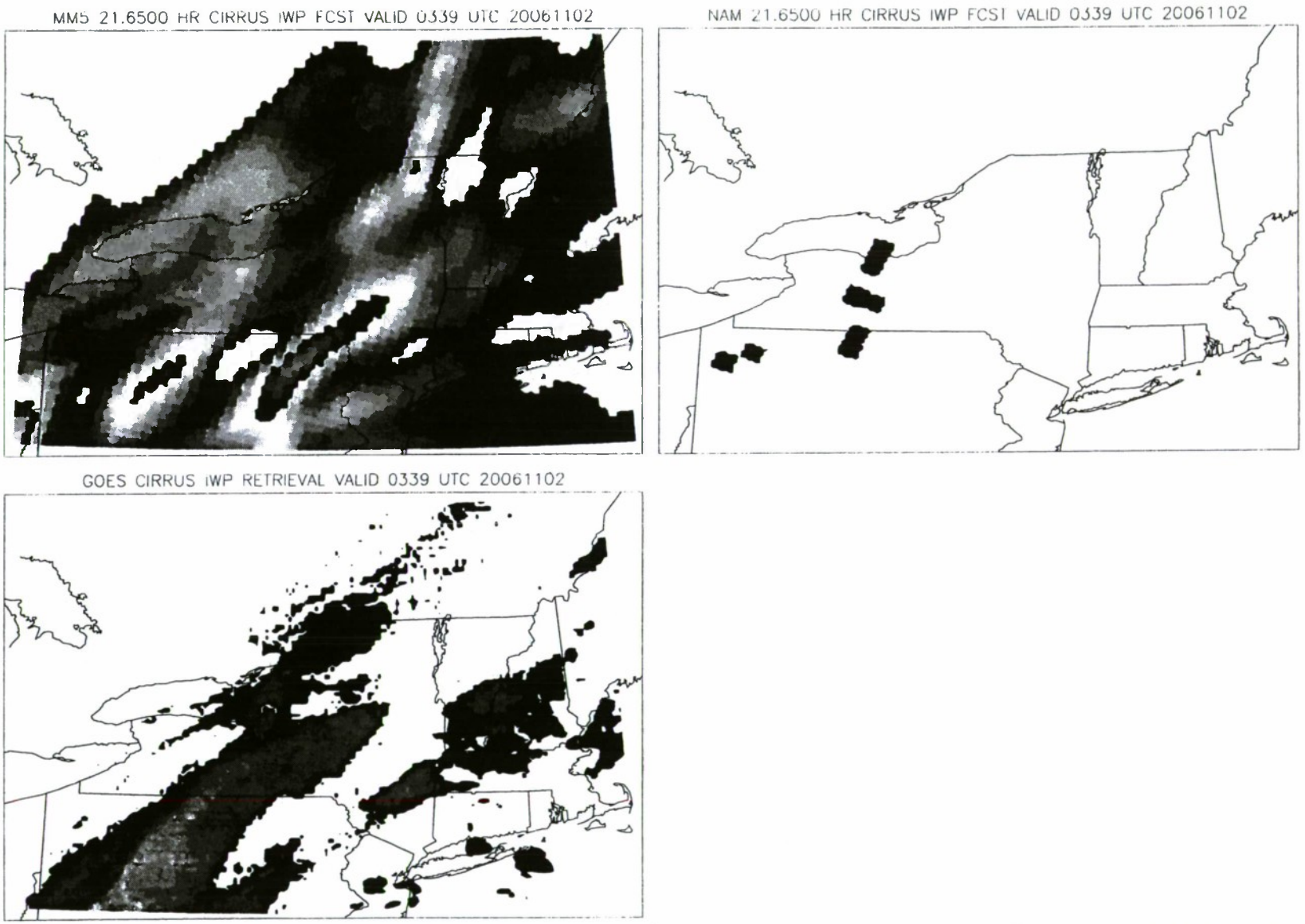

Figure 2. Same as in Figure 1 except ice water path (g m^{-2}). Gray scale interval is 25 g m^{-2} starting with black at 25 g m^{-2}.

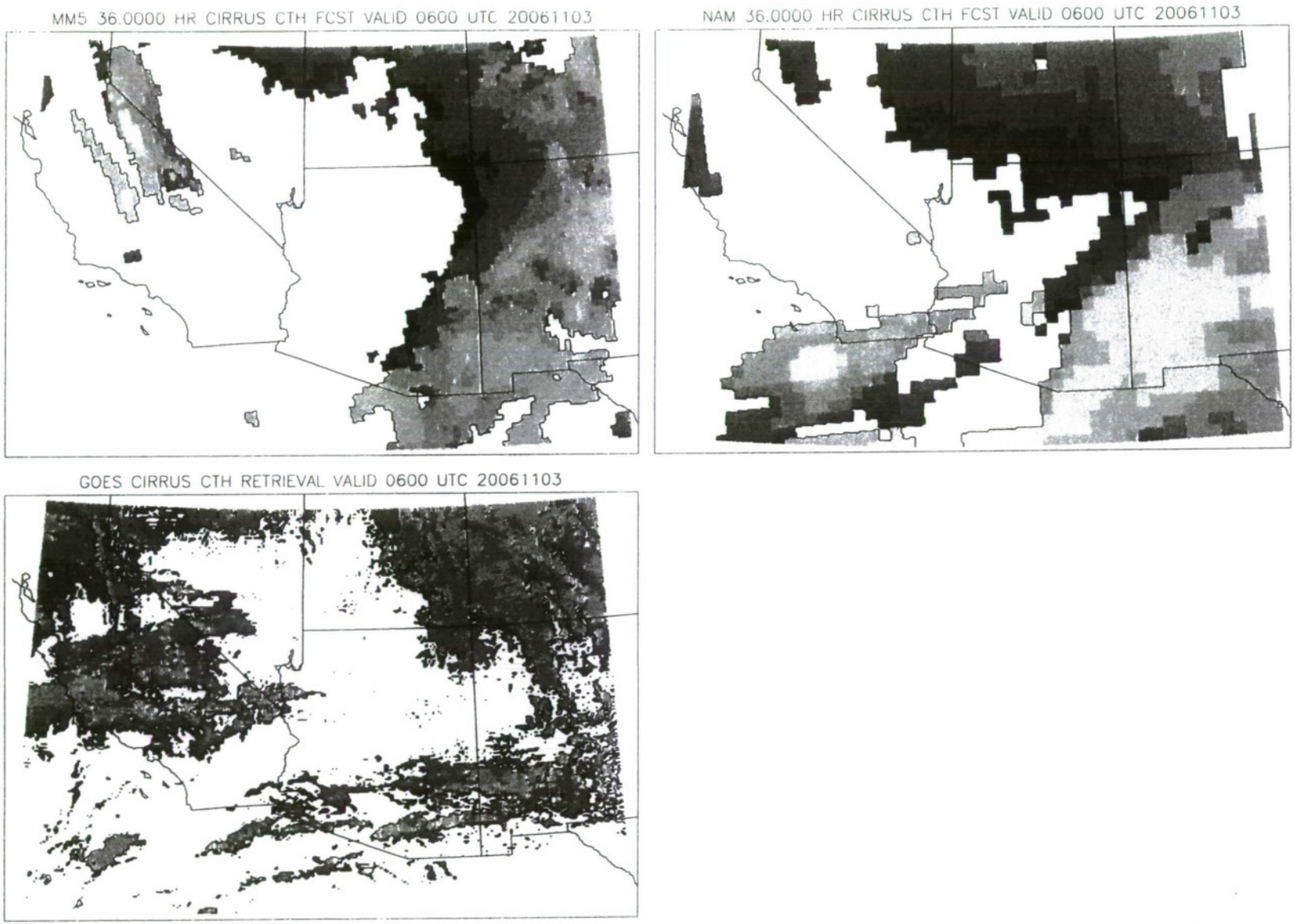

Figure 3. SWUS cirrus top height (km) valid at 0600 UTC 3 November 2006 from 36-h MM5, NAM forecasts and GOES-11 analysis as labeled. Gray scale intevals are 1 km starting with black shading at 6 km.

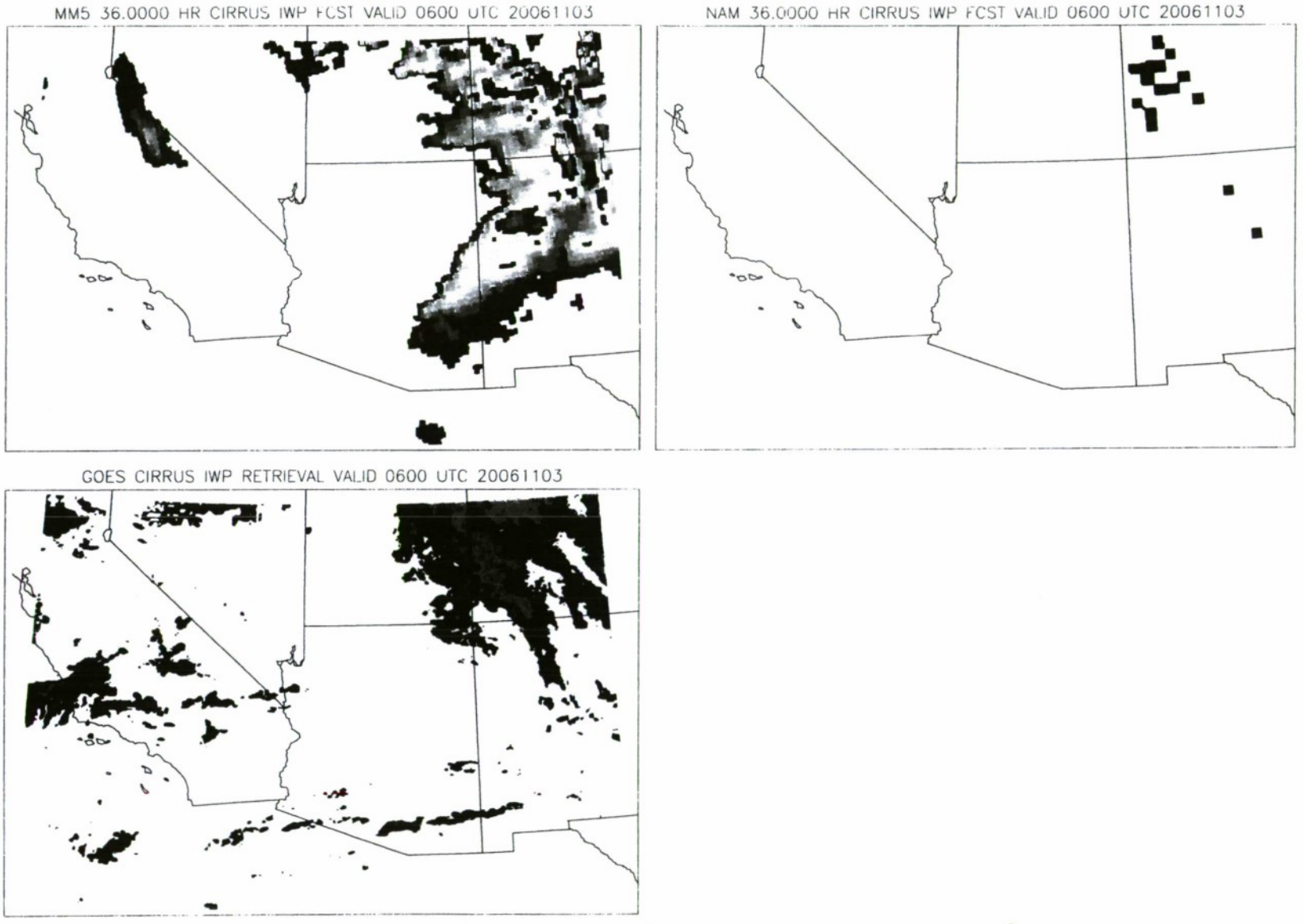

Figure 4. Same as in Figure 3 except ice water path (g m^{-2}). Gray scale interval is 25 g m^{-2} starting with black at 25 g m^{-2}.

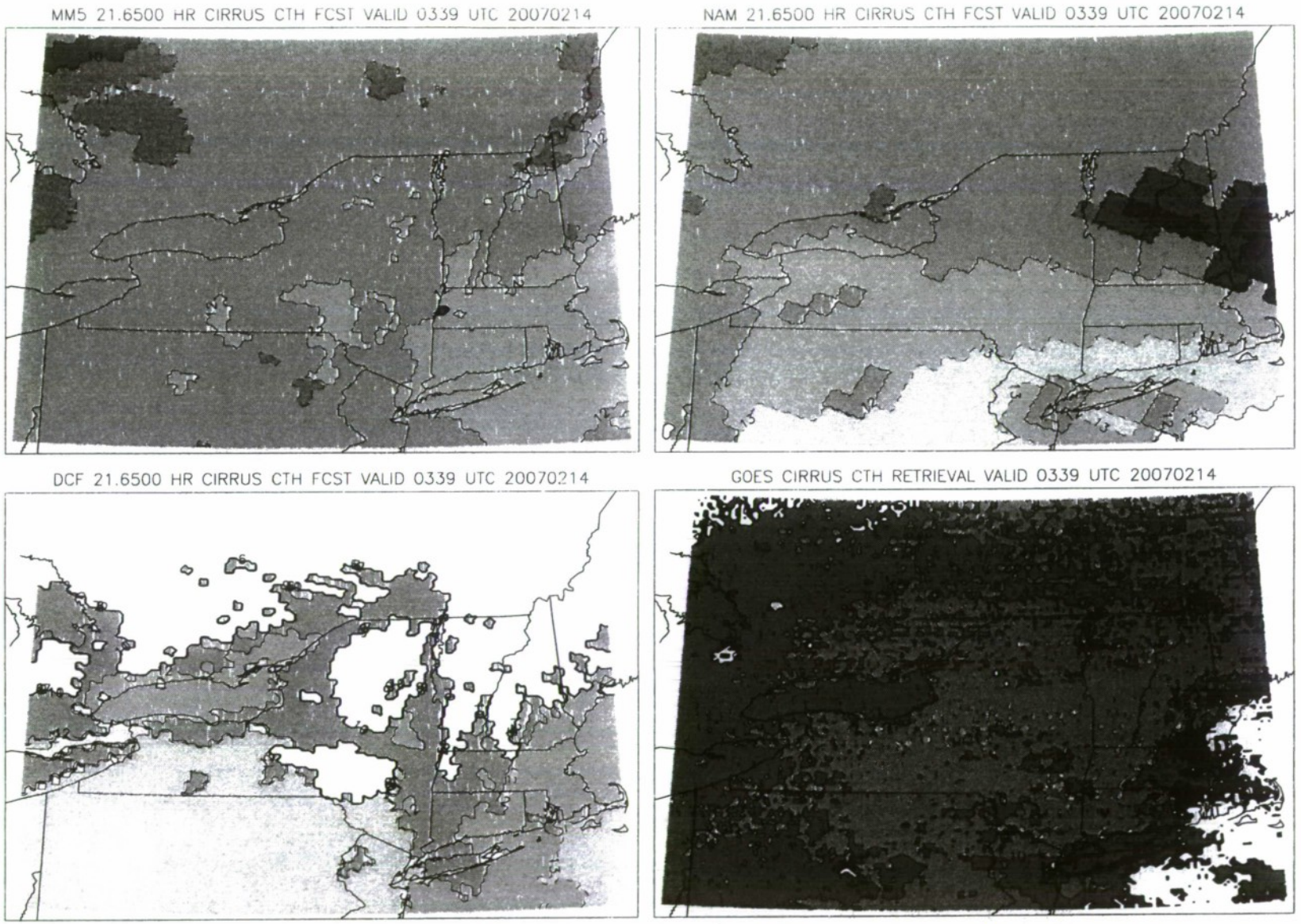

Figure 5. NEUS cirrus top height (km) valid 0339 UTC 14 February 2007 from 21.65-h MM5, NAM, DCF forecasts and GOES-12 analysis as labeled. Contour and gray scale intervals are 1 km.

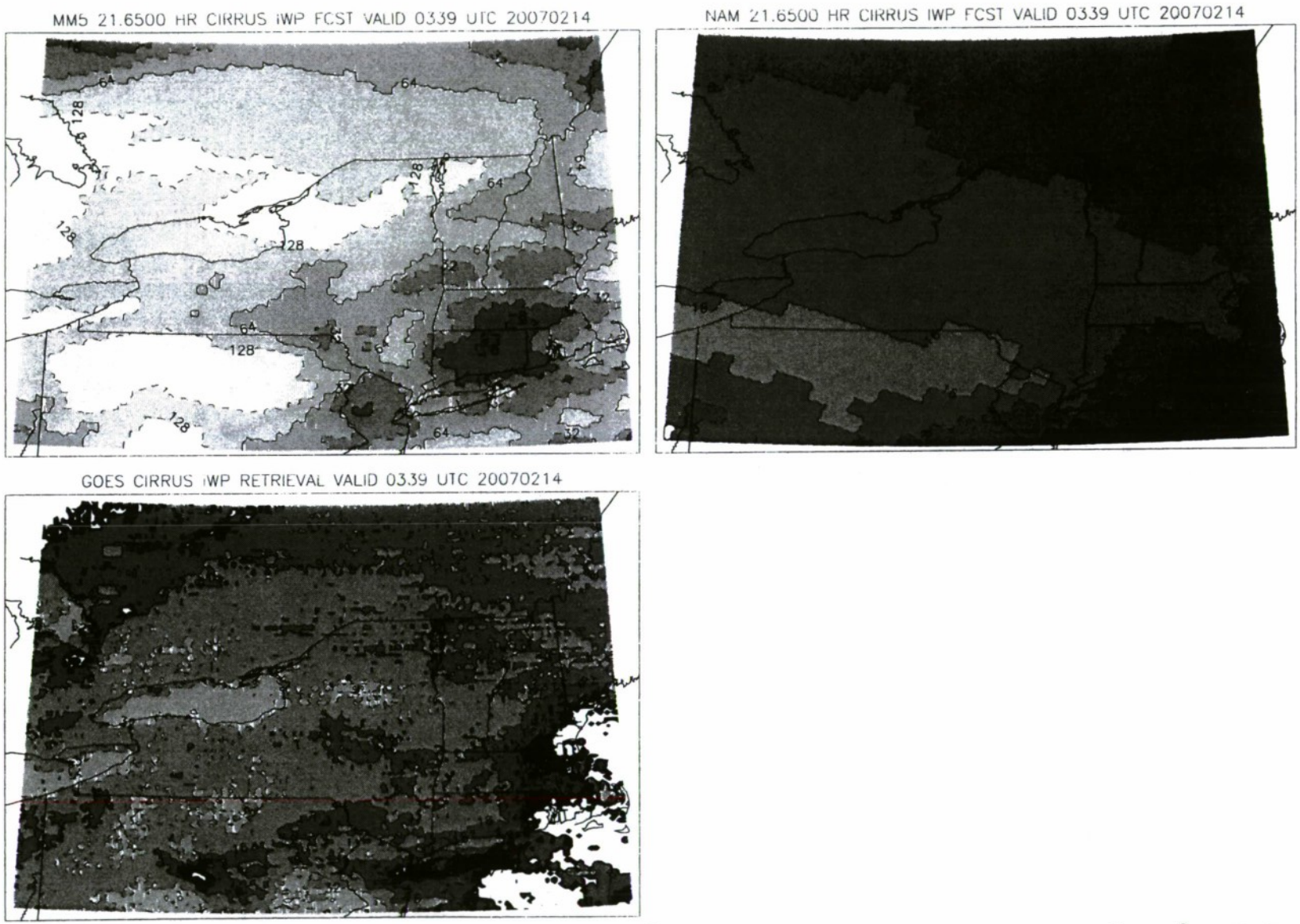

Figure 6. Same as in Figure 5 except ice water path (g m^{-2}). Contour and gray scale intervals are 2^n g m^{-2}, n=0, 9.

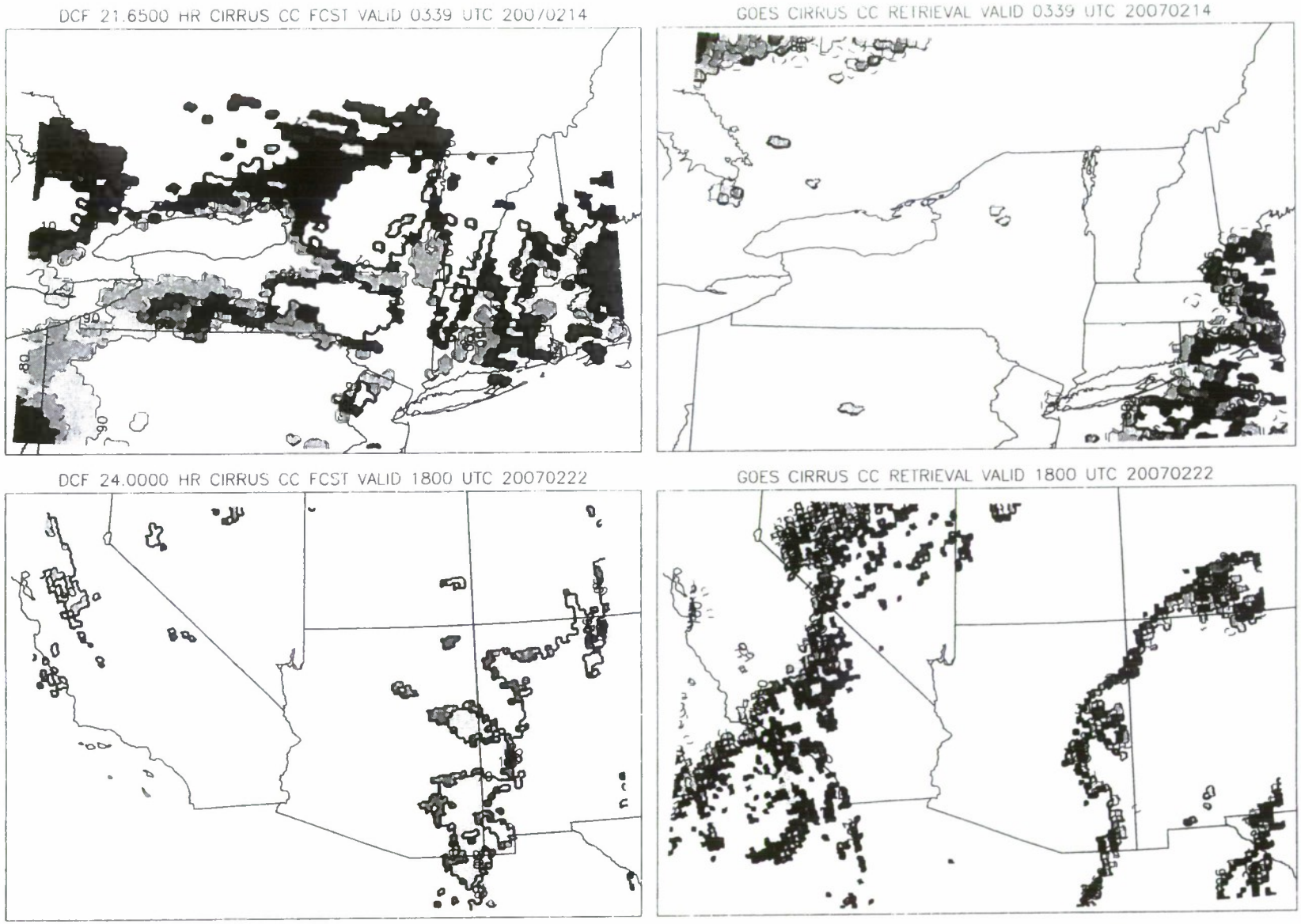

Figure 7. Cirrus cover (%) from NEUS 21.65-h DCF forecast and GOES-12 analysis valid 0339 UTC 14 February 2007, and from SWUS 24-h DCF forecast and GOES-11 analysis valid 1800 UTC 22 February 2007. Contour interval is 10%.

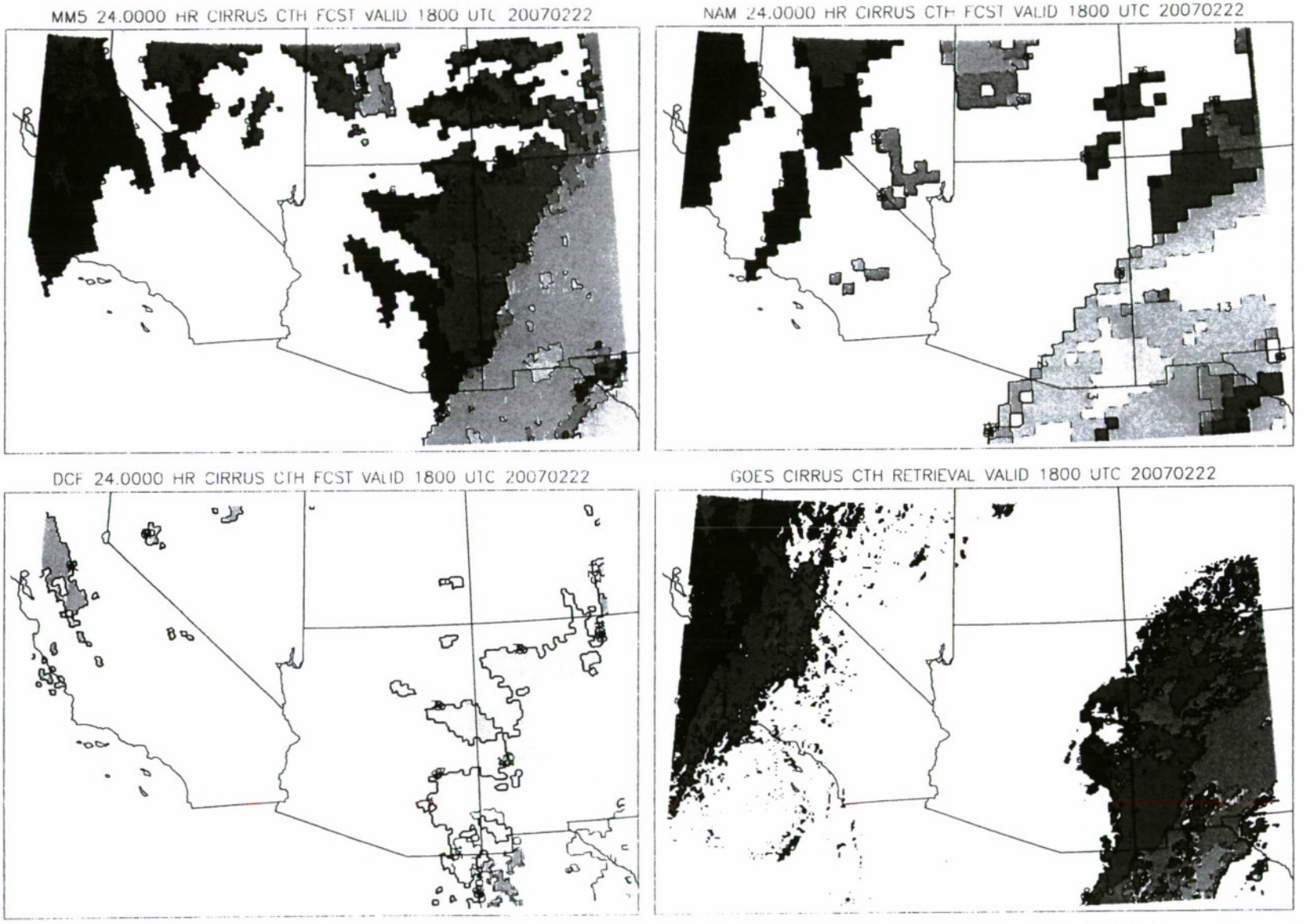

Figure 8. SWUS cirrus top height (km) valid 1800 UTC 22 February 2007 from 24-h MM5, NAM, DCF forecasts and GOES-11 analysis as labeled. Contour and gray scale intervals are 1 km.

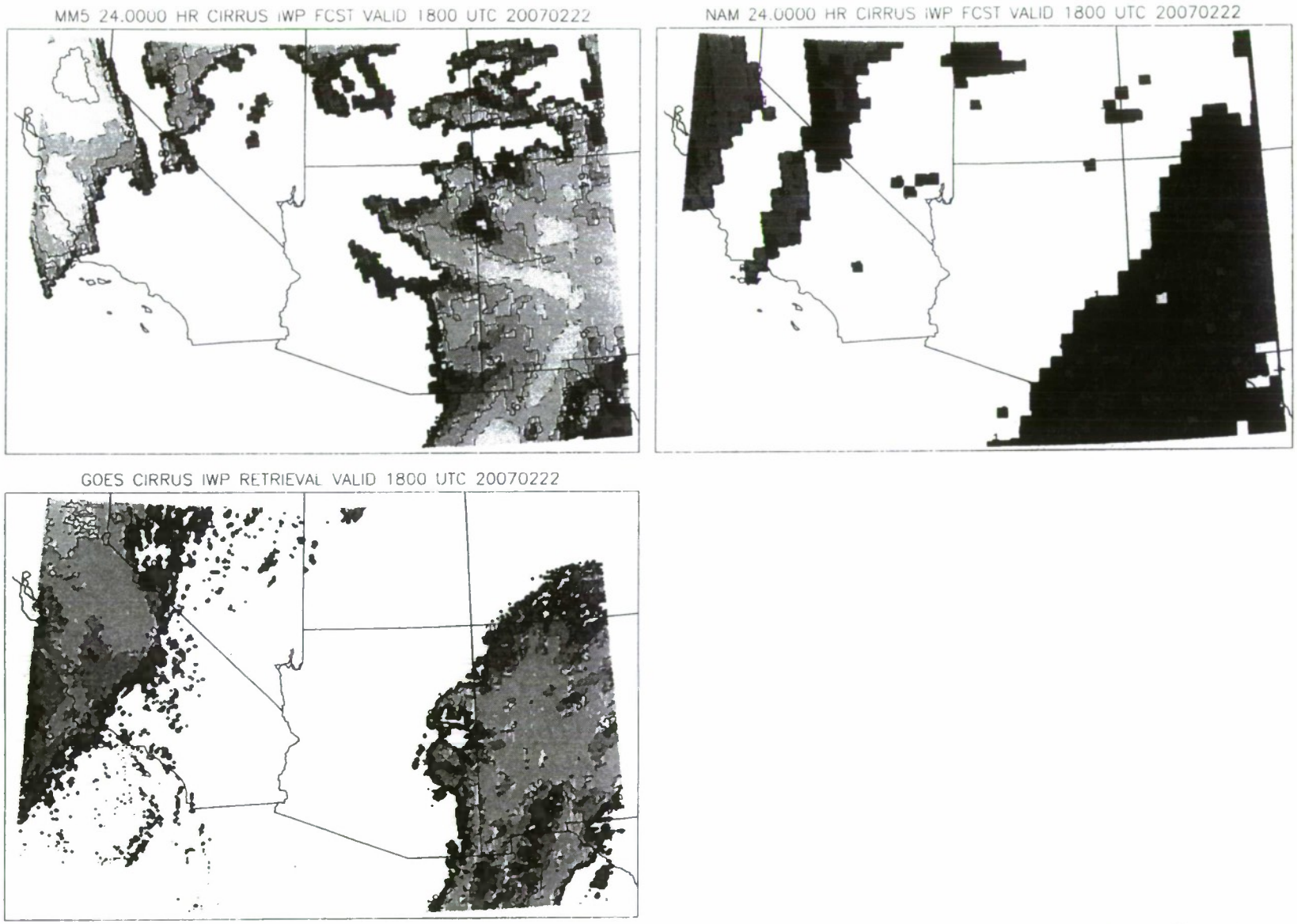

Figure 9. Same as in Figure 8 except ice water path (g m^{-2}). Contour and gray scale intervals are 2^n g m^{-2}, n=0, 9.

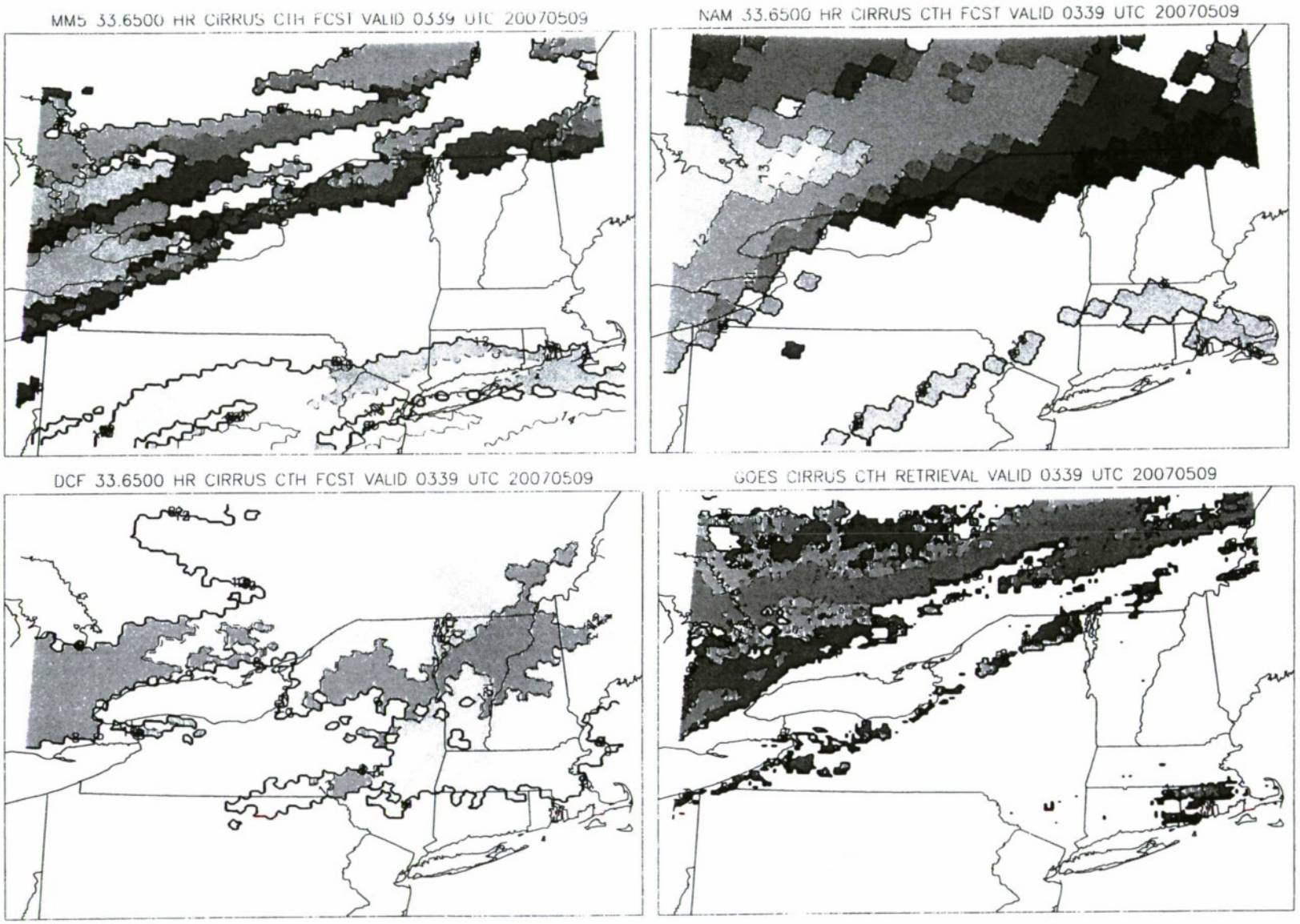

Figure 10. NEUS cirrus top height (km) valid 0339 UTC 9 May 2007 from 35.65-h MM5, NAM, DCF forecasts and GOES-12 analysis as labeled. Contour and gray scale intervals are 1 km.

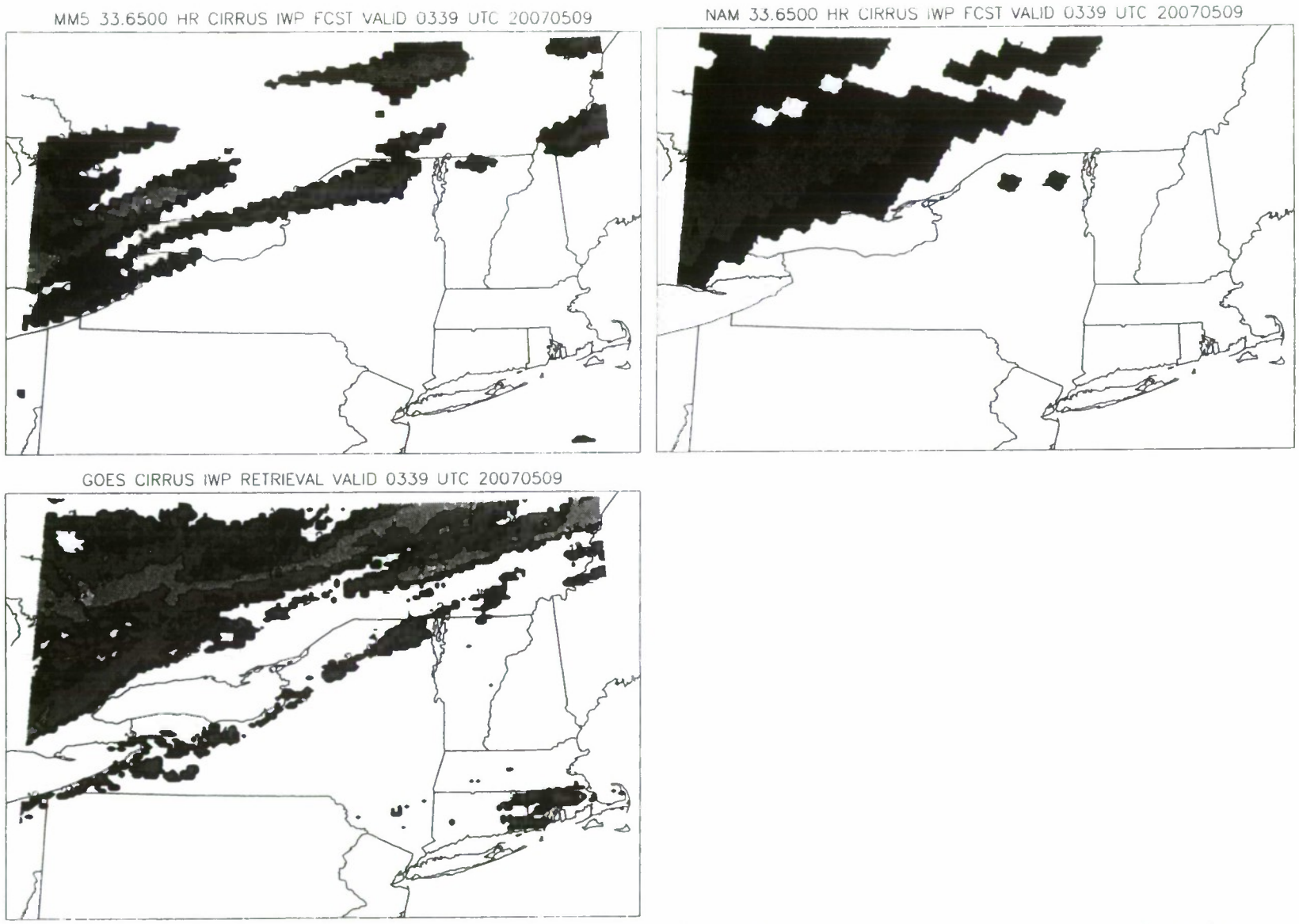

Figure 11. Same as in Figure 10 except ice water path (g m^{-2}). Contour and gray scale intervals are 2^n g m^{-2}, n=0, 9.

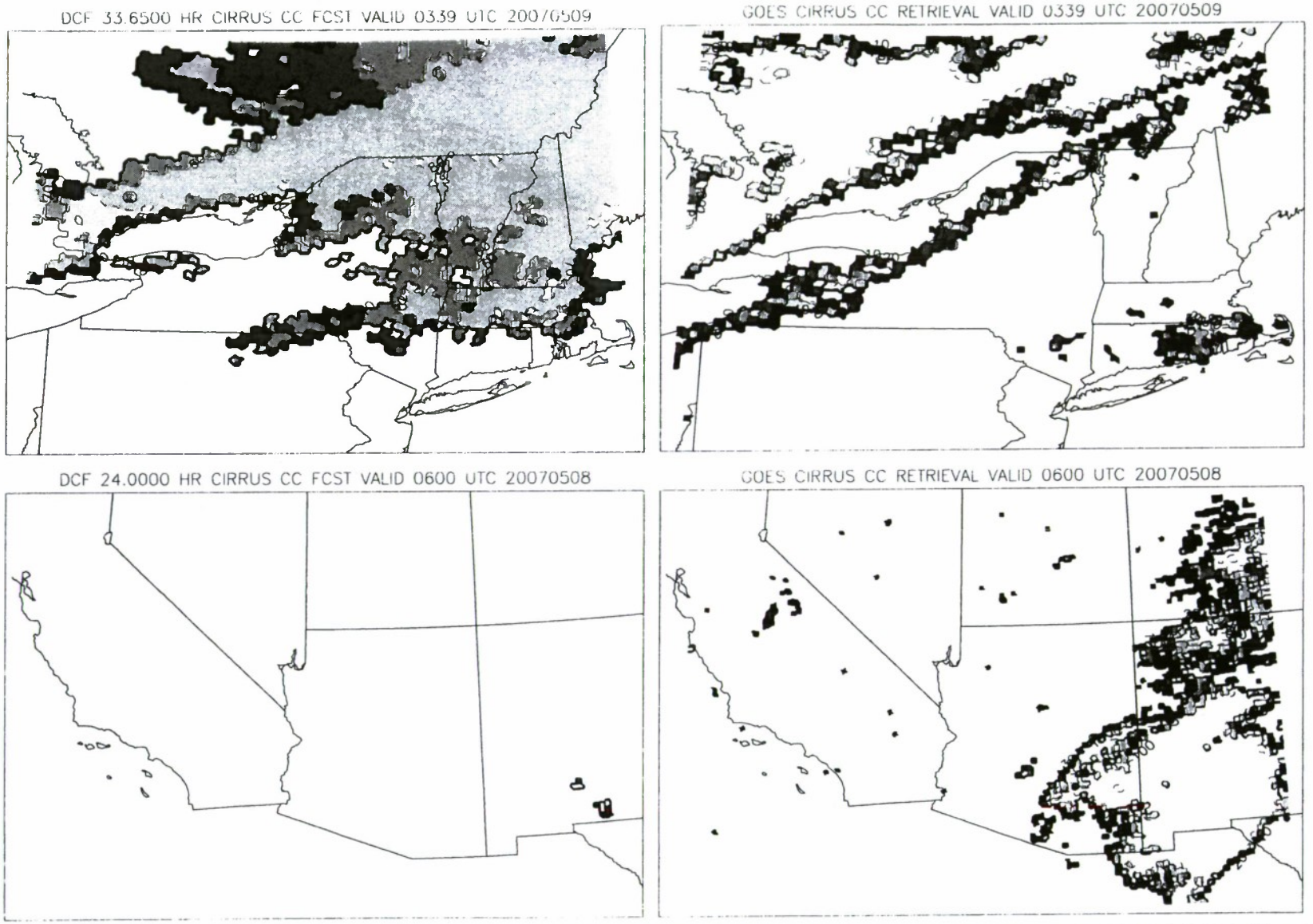

Figure 12. Cirrus cloud cover (%) from NEUS 35.65-h DCF forecast and GOES-12 analysis valid 0339 UTC 9 May 2007, and from SWUS 24-h DCF forecast and GOES-11 analysis valid 0600 UTC 8 May 2007. Contour interval is 10%.

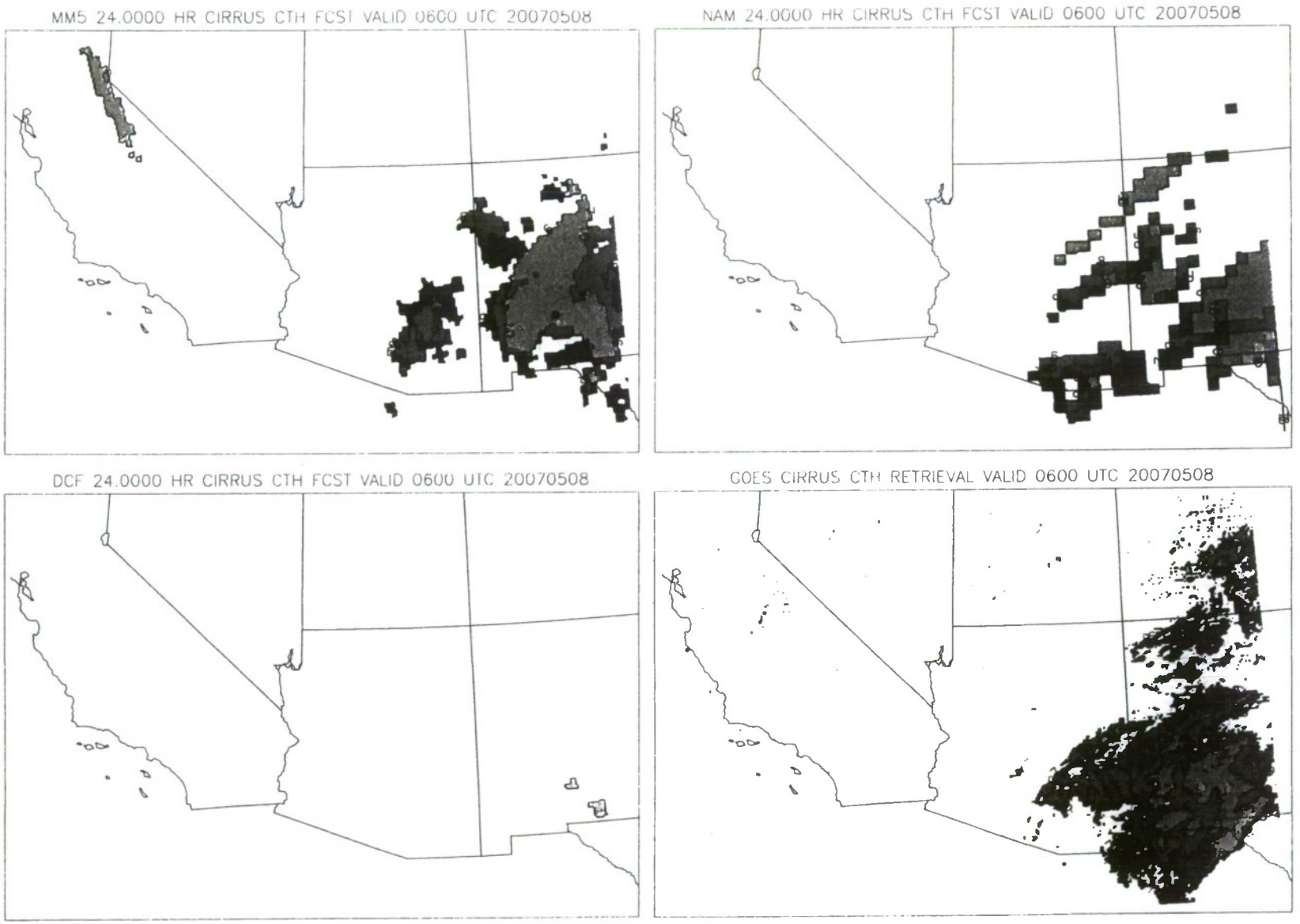

Figure 13. SWUS cirrus top height (km) valid 0600 UTC 8 May 2007 from 24-h MM5, NAM, DCF forecasts and GOES-11 analysis as labeled. Contour and gray scale interval is 1 km.

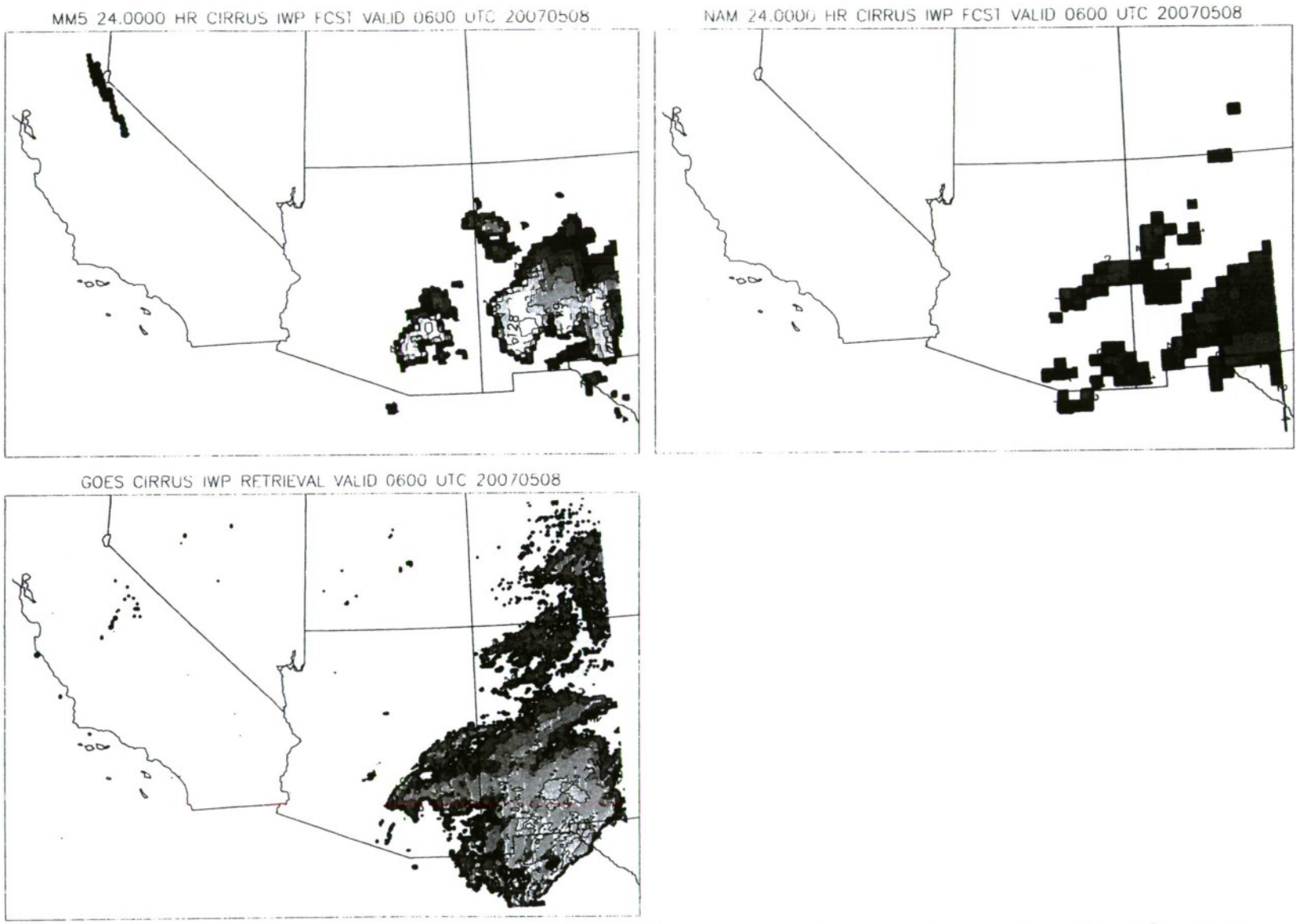

Figure 14. Same as Figure 13 except ice water path (g m^{-2}). Contour and gray scale interval is 2^n g m^{-2}, n=0, 9.

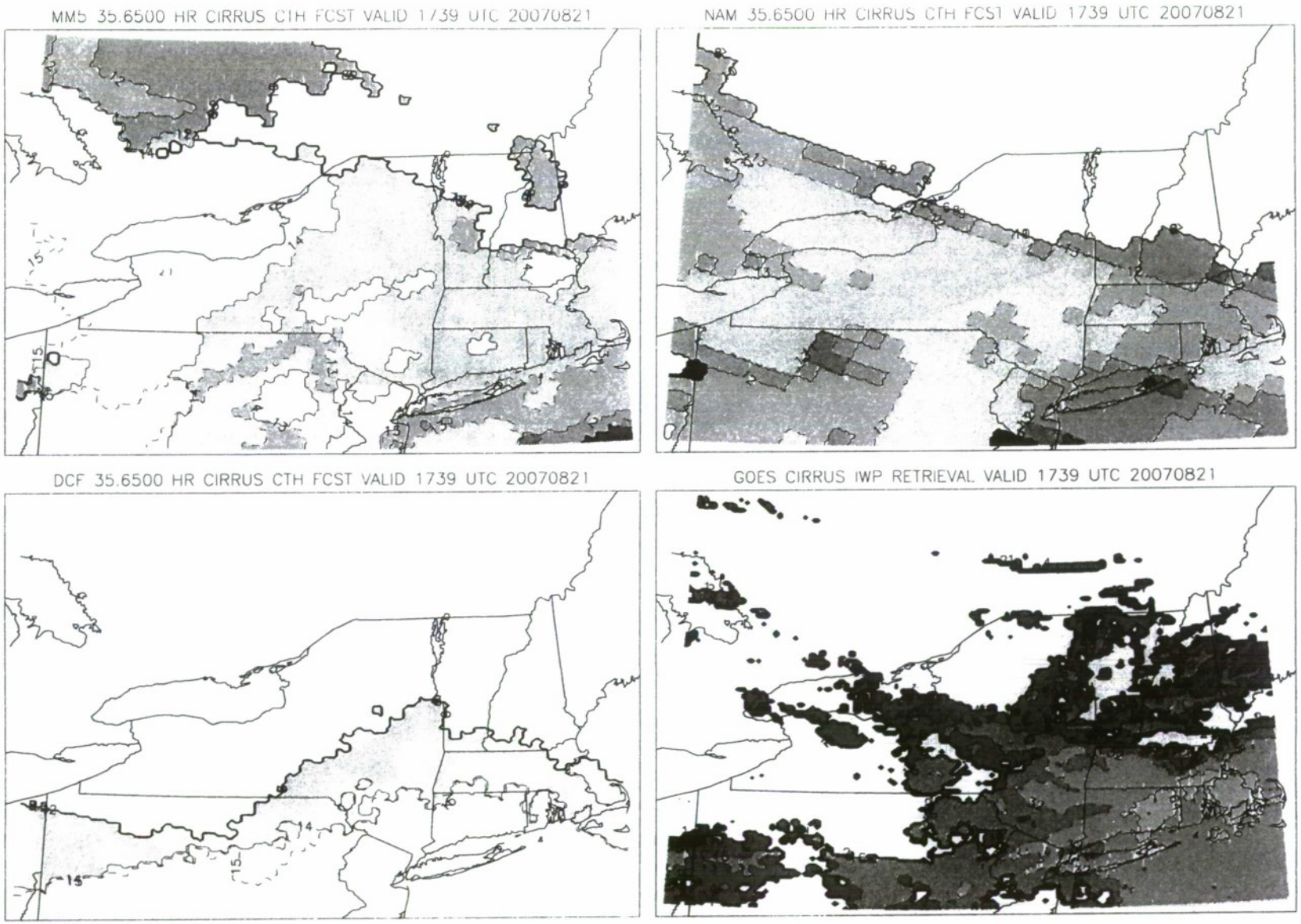

Figure 15. NEUS cirrus top height (km) valid 1739 UTC 21 August 2007 from 35.65-h MM5, NAM, DCF forecasts and GOES-12 analysis as labeled. Contour and gray scale interval is 1 km.

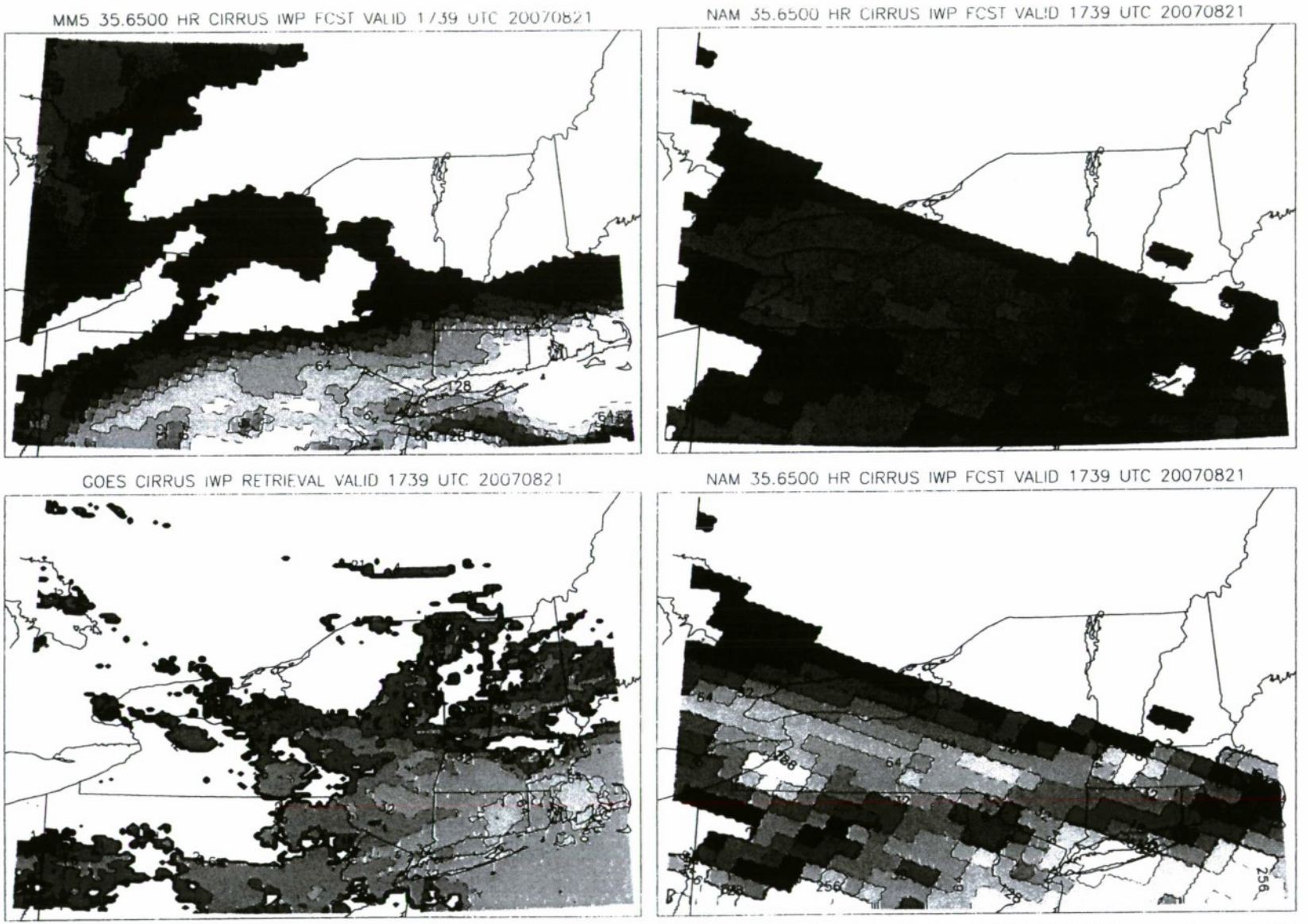

Figure 16. NEUS ice water path (g m^{-2}) valid 1739 UTC 21 August 2007 from 35.65-h MM5, NAM forecasts and GOES-12 analysis. Lower right is NAM forecast of cloud ice mixing ratio plus snow water mixing ratio converted to ice water path.

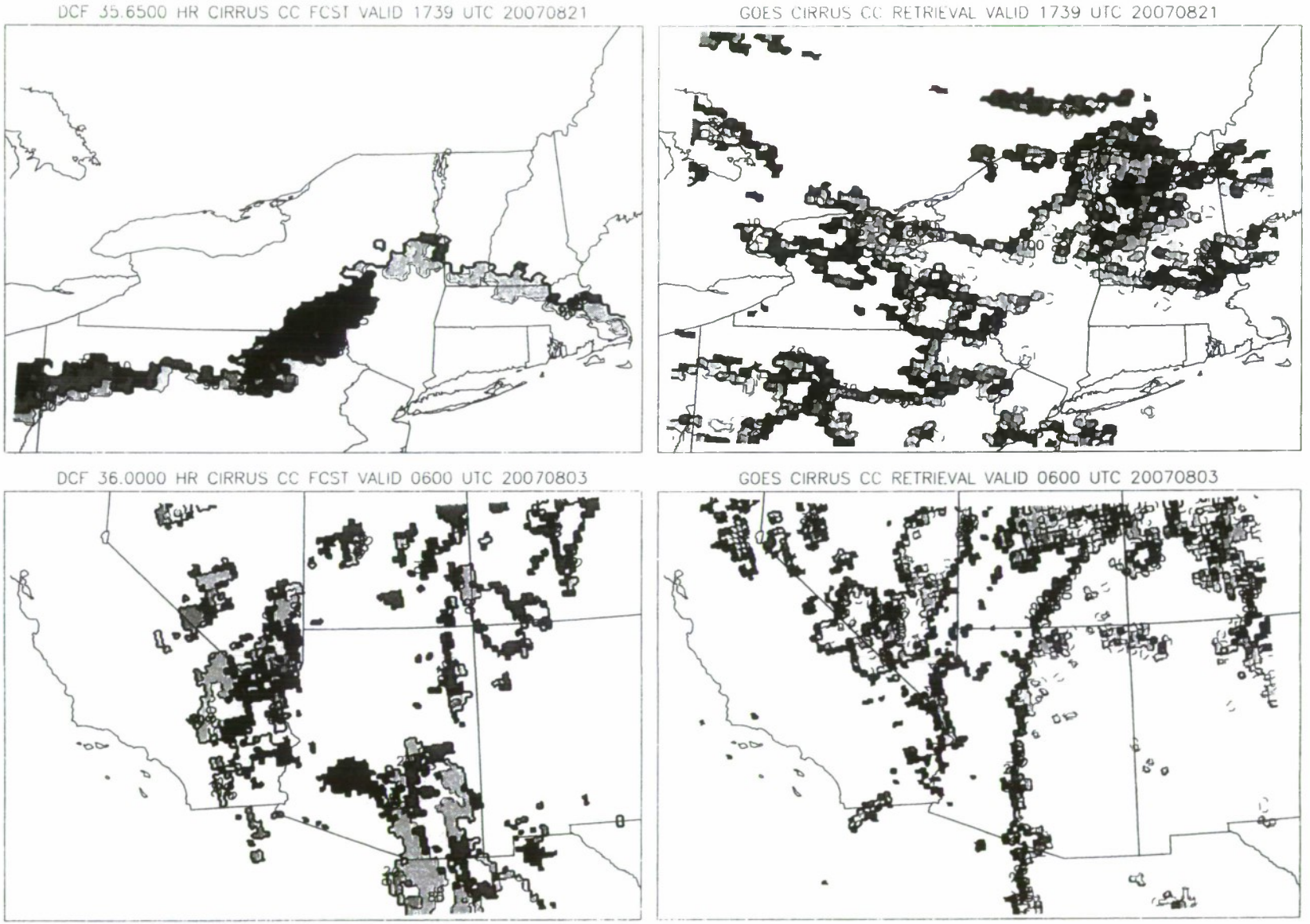

Figure 17. Cirrus cloud cover (%) from NEUS 35.65-h DCF forecast and GOES-12 analysis valid 1739 UTC 21 August 2007, and from SWUS 36-h DCF forecast and GOES-11 analysis valid 0600 UTC 3 August 2007. Contour interval is 10%.

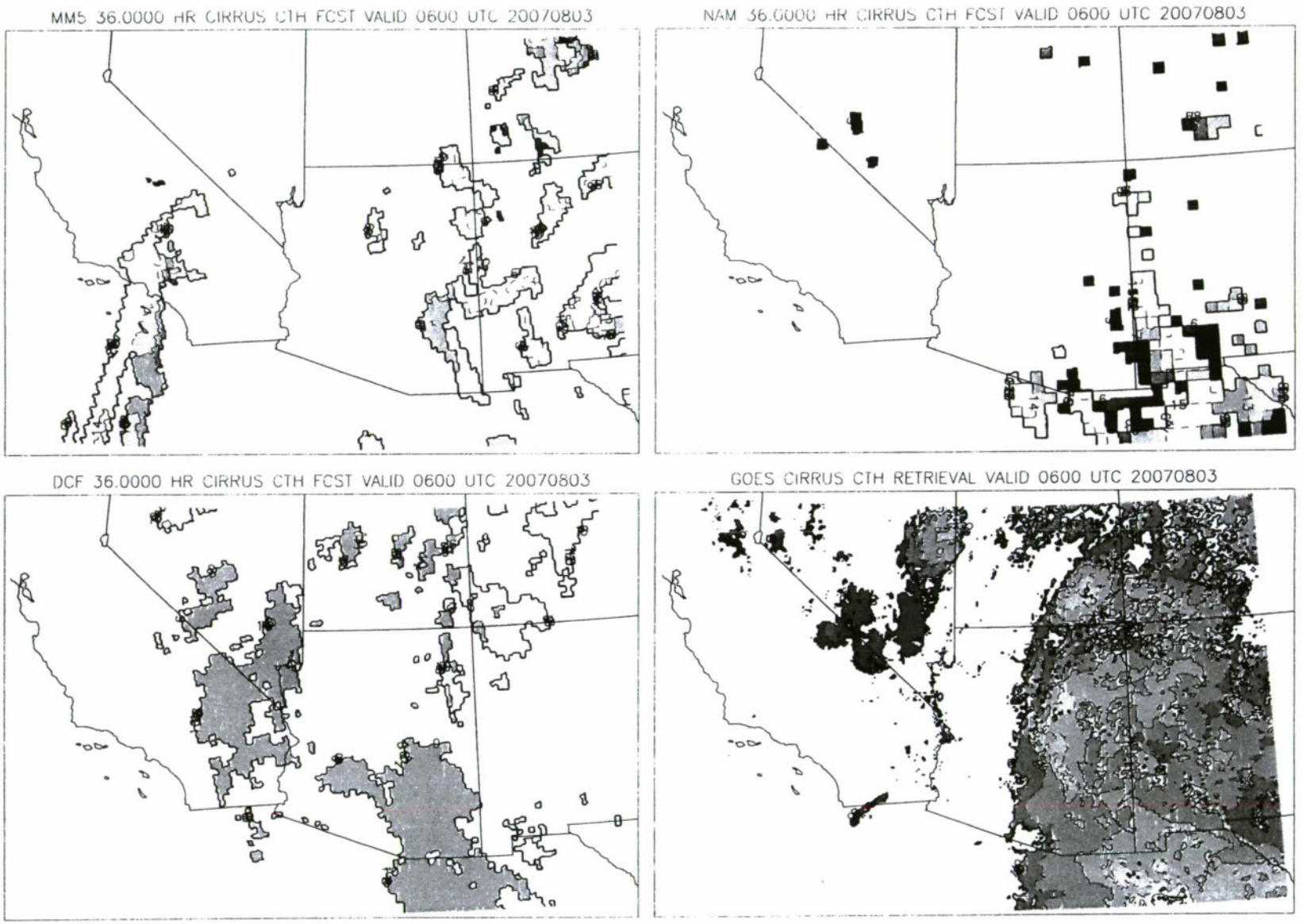

Figure 18. SWUS cirrus top height (km) valid 0600 UTC 3 August 2007 from 36-h MM5, NAM, DCF forecasts and GOES-11 analysis as labeled. Contour and gray scale interval is 1 km.

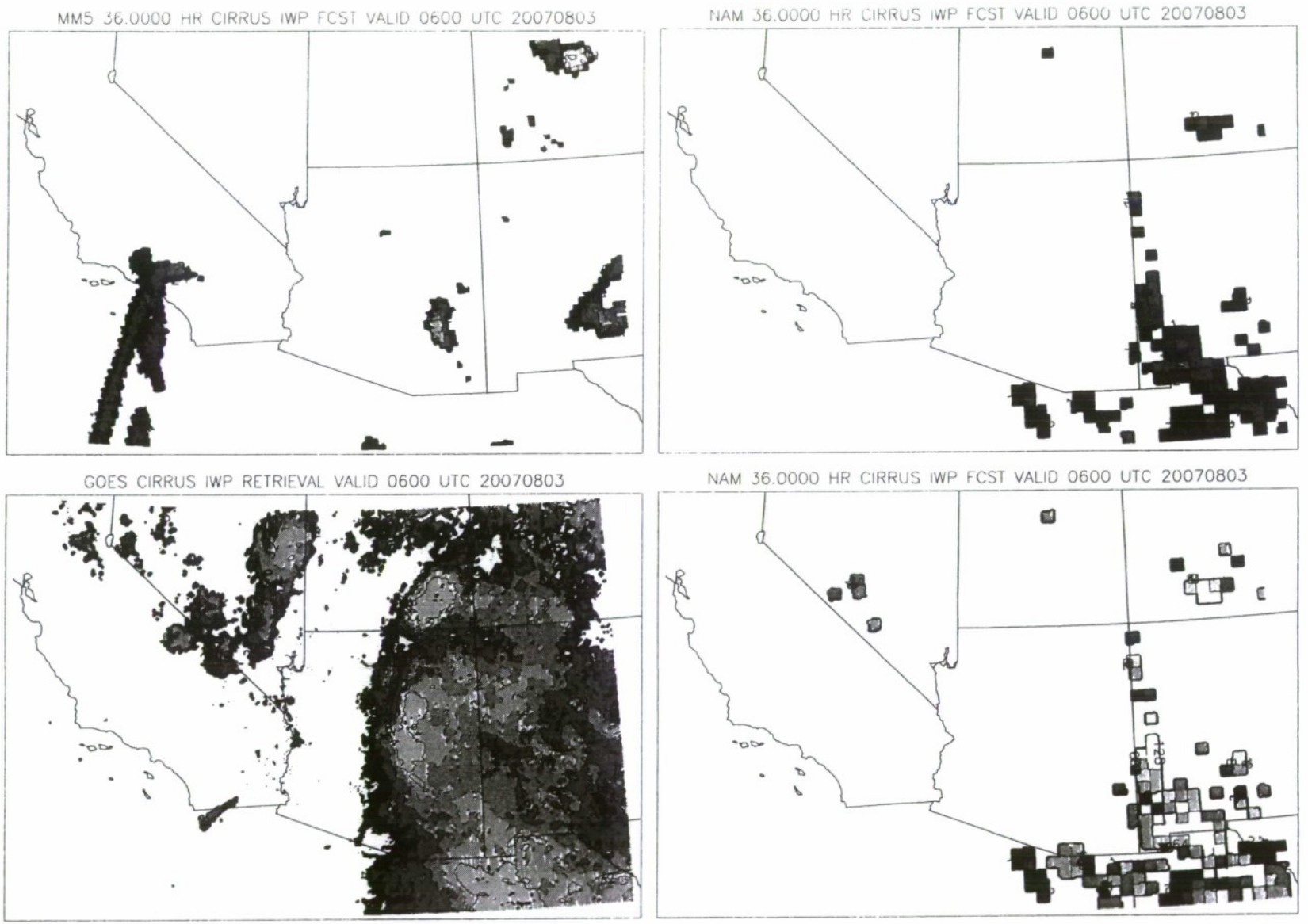

Figure 19. SWUS ice water path (g m^{-2}) valid 0600 UTC 3 August 2007 from 36-h MM5, NAM forecasts and GOES-11 analysis. Lower right is NAM forecast of cloud ice mixing ratio plus snow water mixing ratio converted to ice water path.

These depictions are shown as examples of selected forecasts and are not intended as a means of objectively assessing forecast performance.

Some issues arise from these figures that are worth noting. First, there is much more spatial scatter and irregularity in the GOES depictions that in the predictions. While this is to be expected to some degree because of the greater spatial resolution of the GOES, it should be recognized that the predictive models/algorithm cannot reproduce all of the fine detail of the cirrus apparent in nature. The most that can be expected of the modeling techniques is that they create ice clouds generally in the locations where the greatest concentrations of cirrus actually occur. Second, it is clear in many cases that the extent of area coverage is less in IWP depictions than is indicated by CTH. A good example of this can be seen in the comparisons of the MM5 maps in Figures 10 and 11, in which CTH indicators of cirrus presence depict a band of cirrus across the southern portion of the region that does not appear in the IWP map. This is because the MM5 IWP values for this band fell below 1 g m^{-2} and did not get plotted on the IWP map. The GOES algorithm did not detect the southern cirrus band, but because we know that very thin cirrus are often not detected by the GOES algorithm, we can't say for sure that there are actually no cirrus present in the southern part of the region. This suggests some level of uncertainty in the evaluation of the cirrus predictions due to the limitation of the reference that is being used, the GOES detection process. Because the satellite algorithm can under-detect cirrus but not over-detect it, a model/algorithm under-prediction is of greater concern than an over-prediction.

4.2 Seasonal Period Summary Statistics

Tables 1-4 show summary statistics for the model/algorithm – GOES

comparisons for both regions and both 24- and 36-hour forecast durations in the Fall, Winter, Spring and Summer periods respectively. The much larger SWUS has many more model grid points and GOES pixels than does the smaller NEUS region. Relative sizes of the MM5 and DCF (15 km) and NAM (32.5 km) grid cells results in more than four times as many MM5 and DCF grid points than NAM points in each region.

Table 1. Fall period summary statistics for comparison of MM5 and NAM ice cloud predictions (average duration in hours in parentheses) with GOES ice cloud retrievals. Numbers of grid points and pixels shown are the total over all forecasts. The last two columns are the percentages of the total number of grid points or pixels in which ice cloud was predicted or detected respectively.

Region/Fcst Duration	Model	# Fcsts	# Model Grid Pts.	# GOES Pixels	% Model Ice Pts.	% GOES Ice Pixels
NEUS/24 (22.7)	MM5	29	83259	802459	54	29
	NAM	25	16675	694000	48	27
NEUS/36 (34.7)	MM5	29	83259	802459	48	29
	NAM	26	17342	721760	46	28
SWUS/24 (24.0)	MM5	62	458738	4306892	26	28
	NAM	58	101094	4018936	26	29
SWUS/36 (36.0)	MM5	62	458738	4306892	27	27
	NAM	58	101094	4018936	24	29

Table 2. Winter period summary statistics for comparison of MM5, NAM and DCF ice cloud predictions (average duration in hours in parentheses) with GOES ice cloud retrievals. Numbers of grid points and pixels shown are the total over all forecasts. The last two columns are the percentages of the total number of grid points or pixels in which ice cloud was predicted or detected respectively.

Region/Fcst Duration	Model	# Fcsts	# Model Grid Pts.	# GOES Pixels	% Model Ice Pts.	% GOES Ice Pixels
NEUS/24 (22.6)	MM5	53	152163	1466563	40	21
	NAM	53	35351	1471280	39	21
	DCF	49	140679	1355879	16	22
NEUS/36 (34.6)	MM5	52	149292	1438892	40	20
	NAM	52	34684	1443520	37	20
	DCF	47	134937	1300537	14	21
SWUS/24 (24.0)	MM5	59	436541	4098494	26	25
	NAM	59	102837	4088228	20	25
	DCF	54	398304	3739878	7	27
SWUS/36 (36.0)	MM5	58	429142	4029028	26	25
	NAM	58	101094	4018936	19	25
	DCF	51	376176	3532107	4	26

Table 3. Same as in Table 2 except for the Spring period.

Region/Fcst Duration	Model	# Fcsts	# Model Grid Pts.	# GOES Pixels	% Model Ice Pts.	% GOES Ice Pixels
NEUS/24 (22.7)	MM5	54	155034	1494234	42	33
	NAM	54	36018	1499040	42	32
	DCF	48	137808	1328208	29	32
NEUS/36 (34.7)	MM5	54	155034	1494234	43	31
	NAM	53	35351	1471280	42	31
	DCF	47	134937	1300537	29	31
SWUS/24 (24.0)	MM5	49	362551	3403834	26	21
	NAM	50	87150	3464600	18	20
	DCF	49	361424	3393593	1	21
SWUS/36 (36.0)	MM5	49	362551	3403834	27	21
	NAM	48	83664	3326016	18	21
	DCF	49	361424	3393593	1	21

Table 4. Same as in Table 2 except for the Summer period.

Region/Fcst Duration	Model	# Fcsts	# Model Grid Pts.	# GOES Pixels	% Model Ice Pts.	% GOES Ice Pixels
NEUS/24 (22.6)	MM5	55	157905	1521905	36	26
	NAM	53	35351	1471280	37	27
	DCF	50	143550	1383550	27	27
NEUS/36 (34.6)	MM5	55	157905	1521905	34	26
	NAM	54	36018	1499040	35	26
	DCF	51	146421	1411221	26	27
SWUS/24 (24.0)	MM5	57	421743	3959562	16	22
	NAM	55	95865	3811060	15	21
	DCF	51	376176	3532107	7	22
SWUS/36 (36.0)	MM5	57	421743	3959562	13	22
	NAM	55	95865	3811060	14	22
	DCF	51	376176	3532107	6	22

The last two columns of Tables 1-4 compare the percentages of all model/algorithm grid points (GOES pixels) for which ice cloud with top height ≥ 6 km was predicted (detected). This is the same as the percentage of the region covered by cirrus, averaged over all comparison times. GOES cirrus coverage in the NEUS is greater in the Spring and Summer periods than in the Winter, whereas the opposite is true of the SWUS region. It is not known if this is a usual occurrence or just a

characteristic of the single year studied. In any case, the models are unable to replicate the relative regional coverage of the seasons and regions. NEUS cirrus coverage is over-predicted on average by both MM5 and NAM in both seasons, especially in the Fall and Winter periods. In the SWUS, both models are in good agreement with GOES cirrus coverage in the Fall as is MM5 in the Winter. MM5 over-predicts in the Spring, whereas NAM under-predicts in the Winter and Spring and both models produce significantly less cirrus than detected by GOES in the Summer. DCF cirrus coverage in the NEUS is biased low in the Winter period, slightly low in the Spring but about right in the Summer term. DCF SWUS cirrus coverage is much less than GOES coverage in Winter, Spring and Summer. It is not clear what happened with the DCF in the Spring over the SWUS where on average only a 1% regional coverage of cirrus was predicted. Only in the Winter and Spring periods did the MM5 predict on average greater regional cirrus cover than did NAM in the SWUS. There are no such clear trends between the models in the NEUS regional coverage prediction, except perhaps for a slightly greater prediction for MM5 than NAM in the Fall and Winter.

4.3 Regional Cirrus Coverage by Individual Forecasts

Prediction of the timing of regional cirrus coverage is of great interest to mission planners in providing guidance for system deployment decisions. Figures 20-27 show the percent cirrus coverage of the NEUS and SWUS regions from individual forecasts by the models and algorithm (24-h forecasts) and the GOES analysis for the Fall - Summer periods in turn. Gaps appearing in the line plots shown are due to missing predictions, verifying time GOES analyses, or both. Dash markers are included in some of the plots to indicate the coverage values when gaps prevent connecting lines.

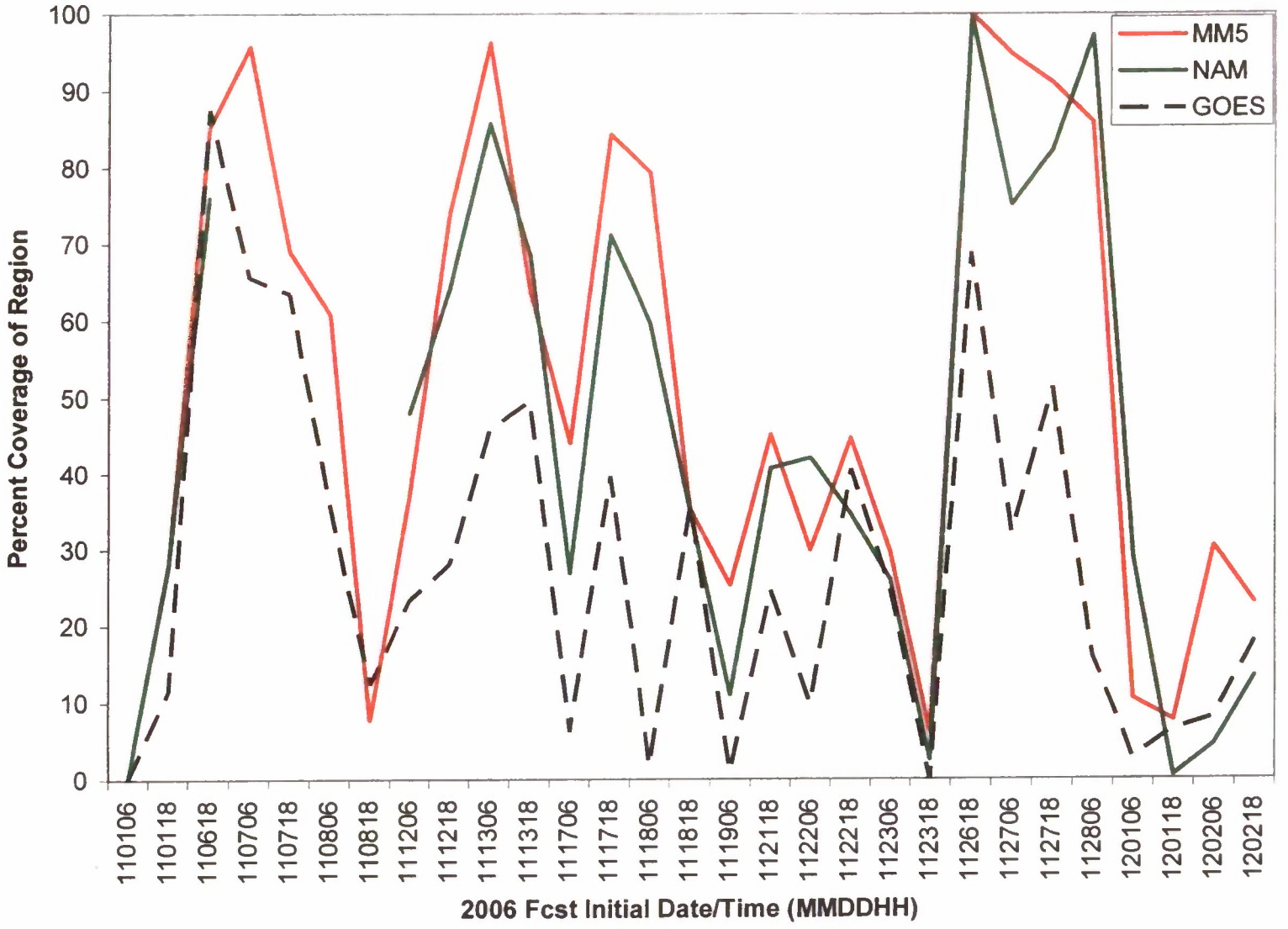

Figure 20. Percent coverage of the NEUS region by MM5 and NAM 24-hour forecast ice cloud grid points and by GOES ice pixels for the Fall period. For each forecast the GOES image at the valid time of the forecast is used.

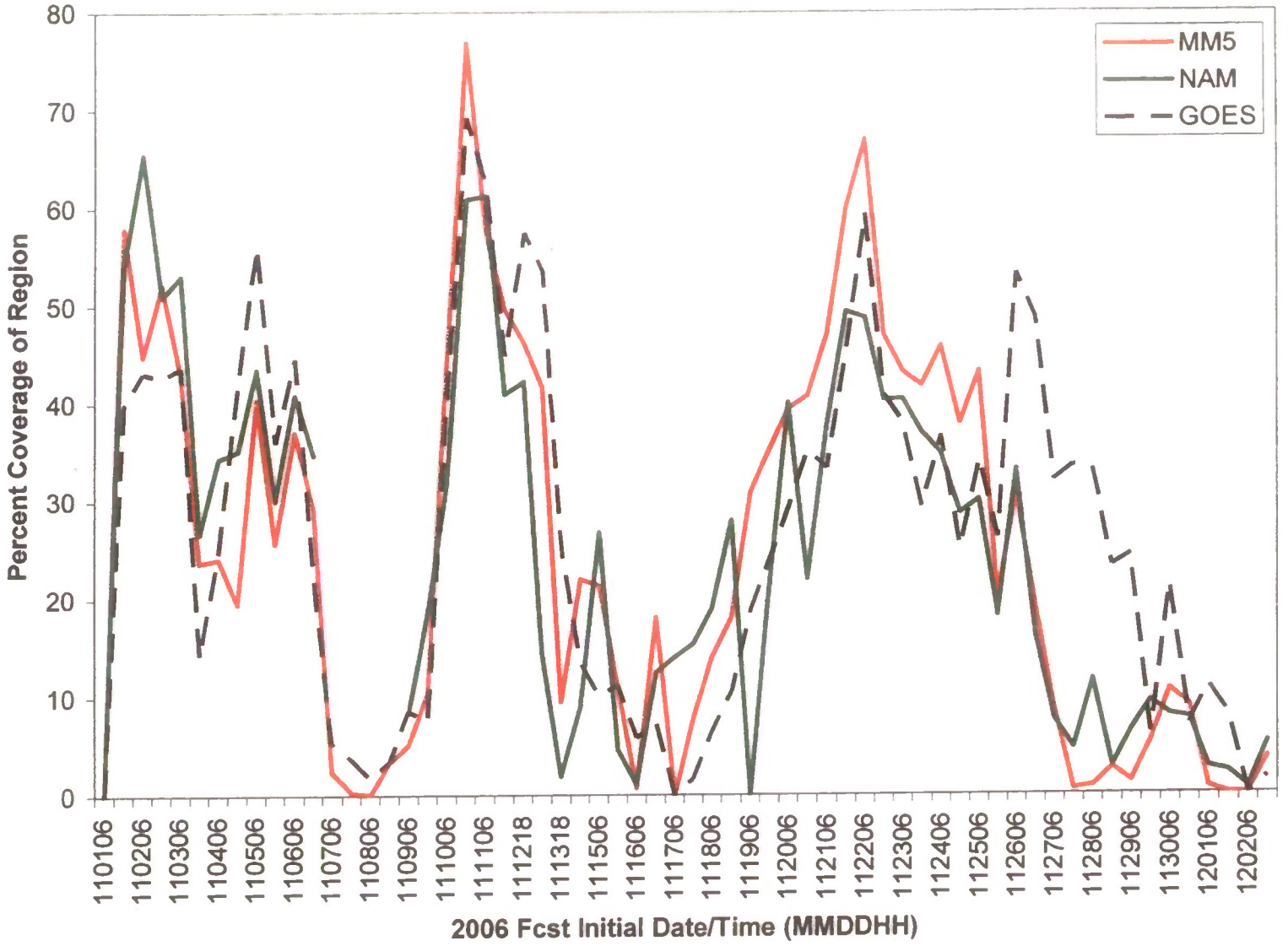

Figure 21. Same as in Figure 20 except for SWUS region.

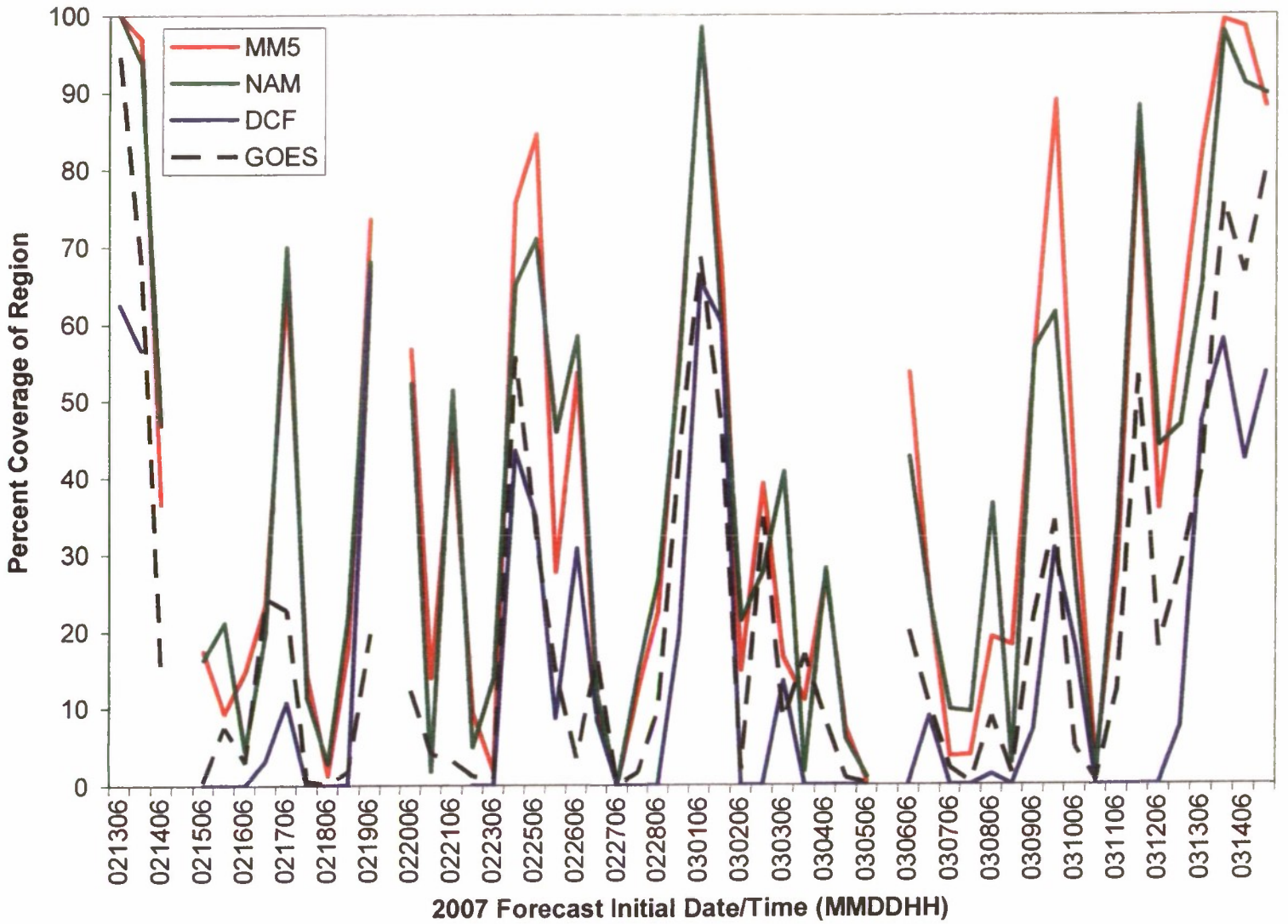

Figure 22. Percent coverage of the NEUS region by MM5, NAM and DCF 24-hour forecast ice cloud grid points and by GOES ice pixels for the Winter period. For each forecast the GOES image at the valid time of the forecast is used.

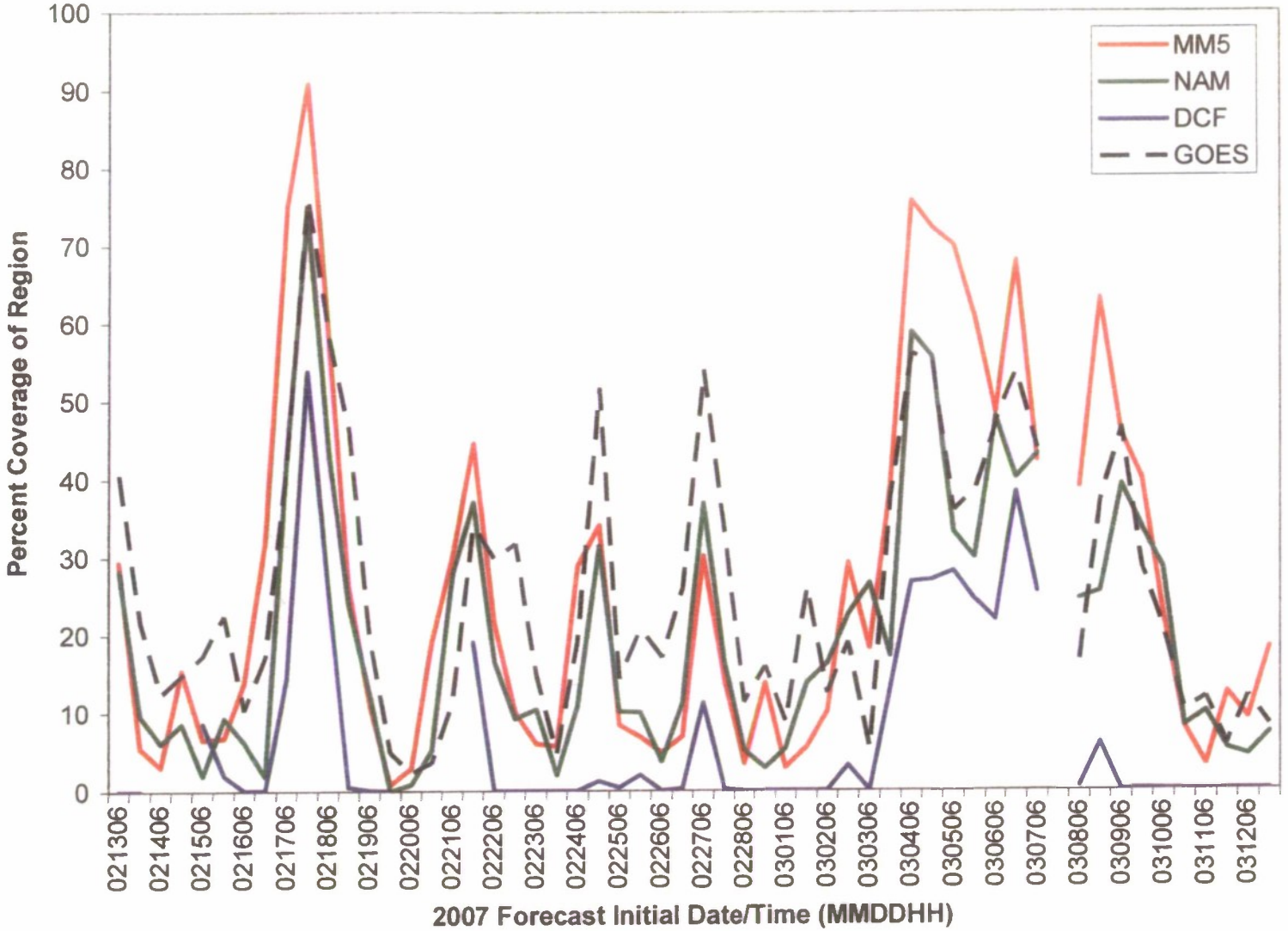

Figure 23. Same as Figure 22 except for SWUS region.

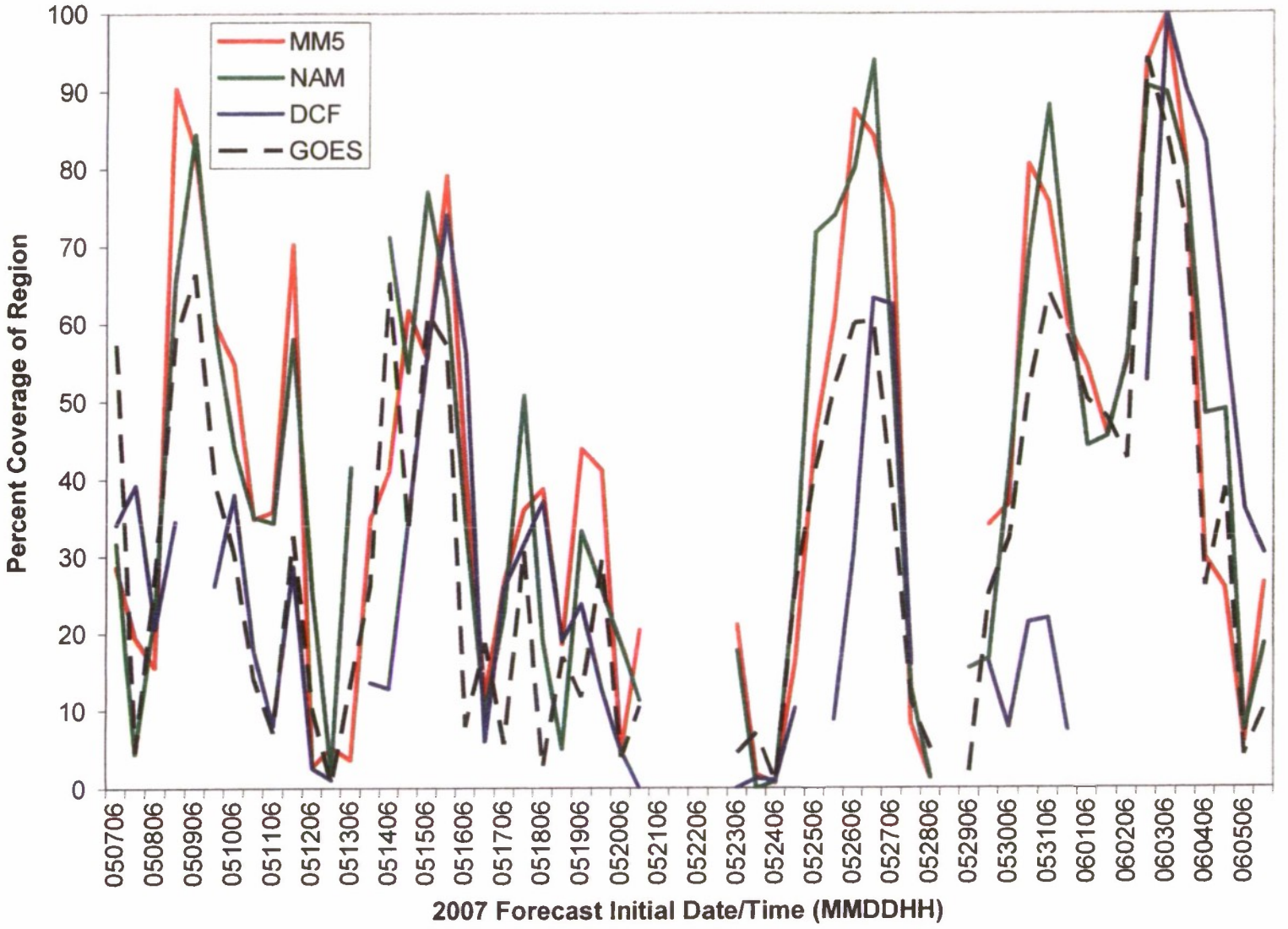

Figure 24. Percent coverage of the NEUS region by MM5, NAM and DCF 24-hour forecast ice cloud grid points and by GOES ice pixels for the Spring period. For each forecast the GOES image at the valid time of the forecast is used.

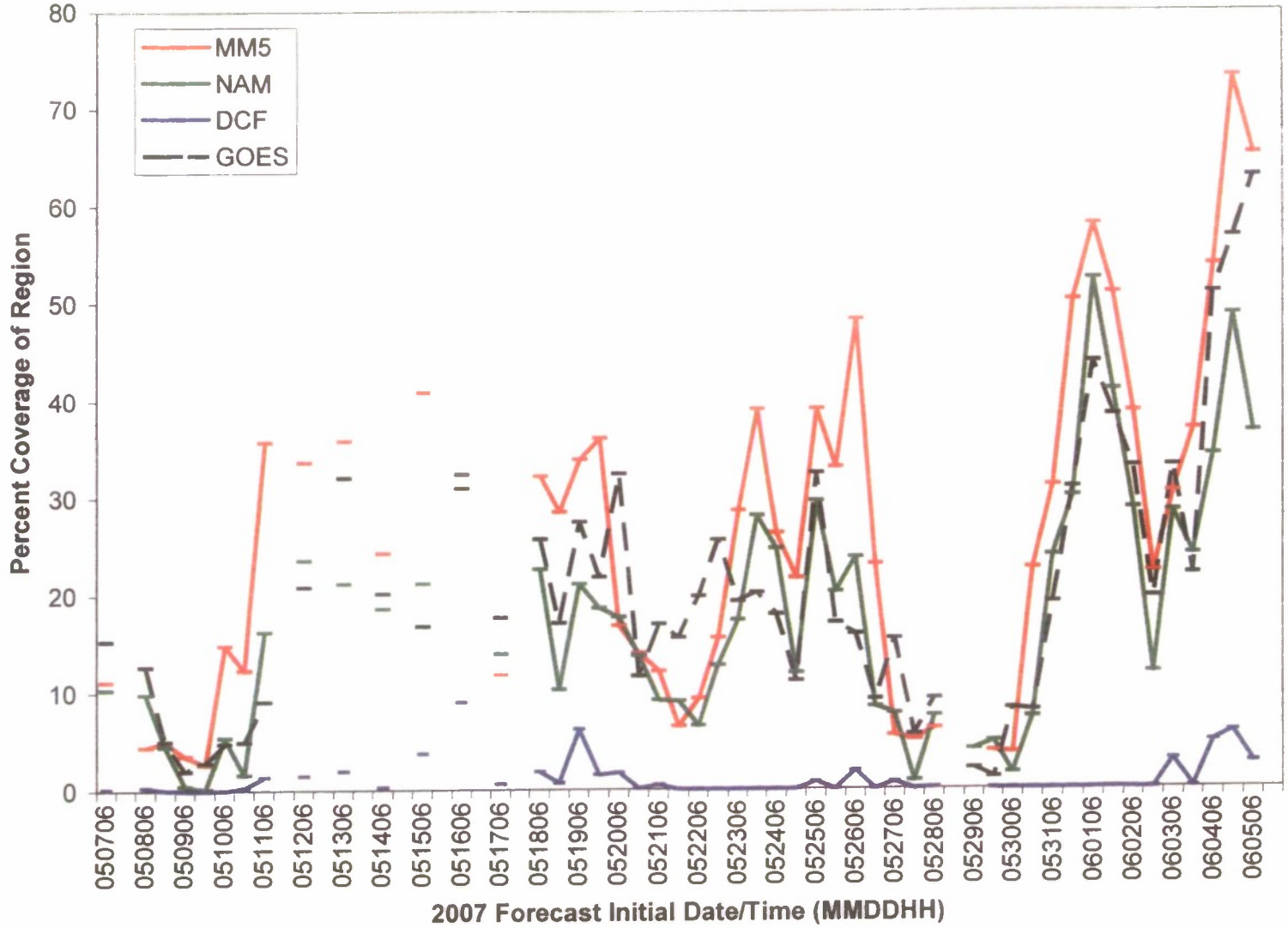

Figure 25. Same as Figure 24 except for SWUS region.

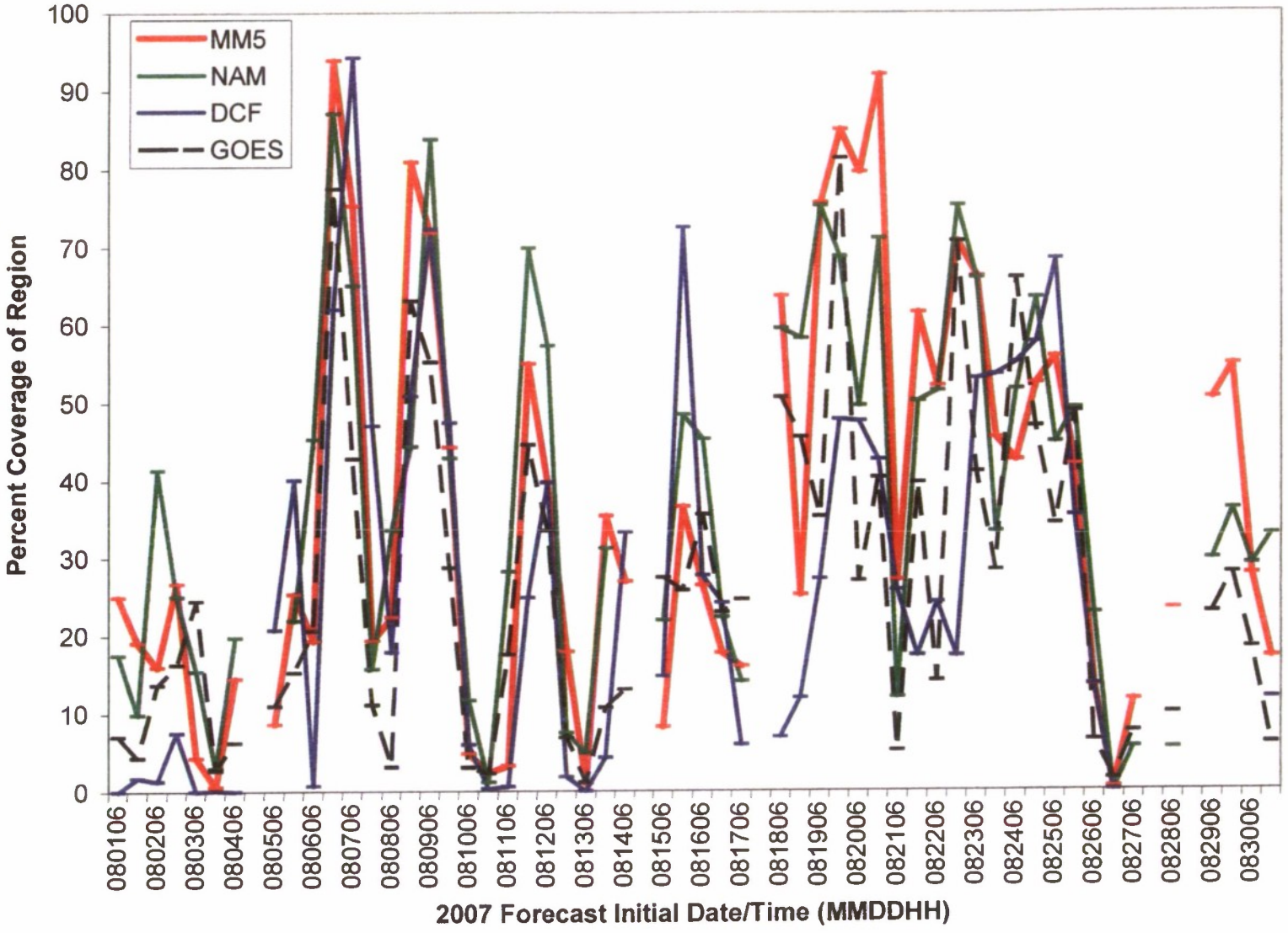

Figure 26. Percent coverage of the NEUS region by MM5, NAM and DCF 24-hour forecast ice cloud grid points and by GOES ice pixels for the Summer period. For each forecast the GOES image at the valid time of the forecast is used.

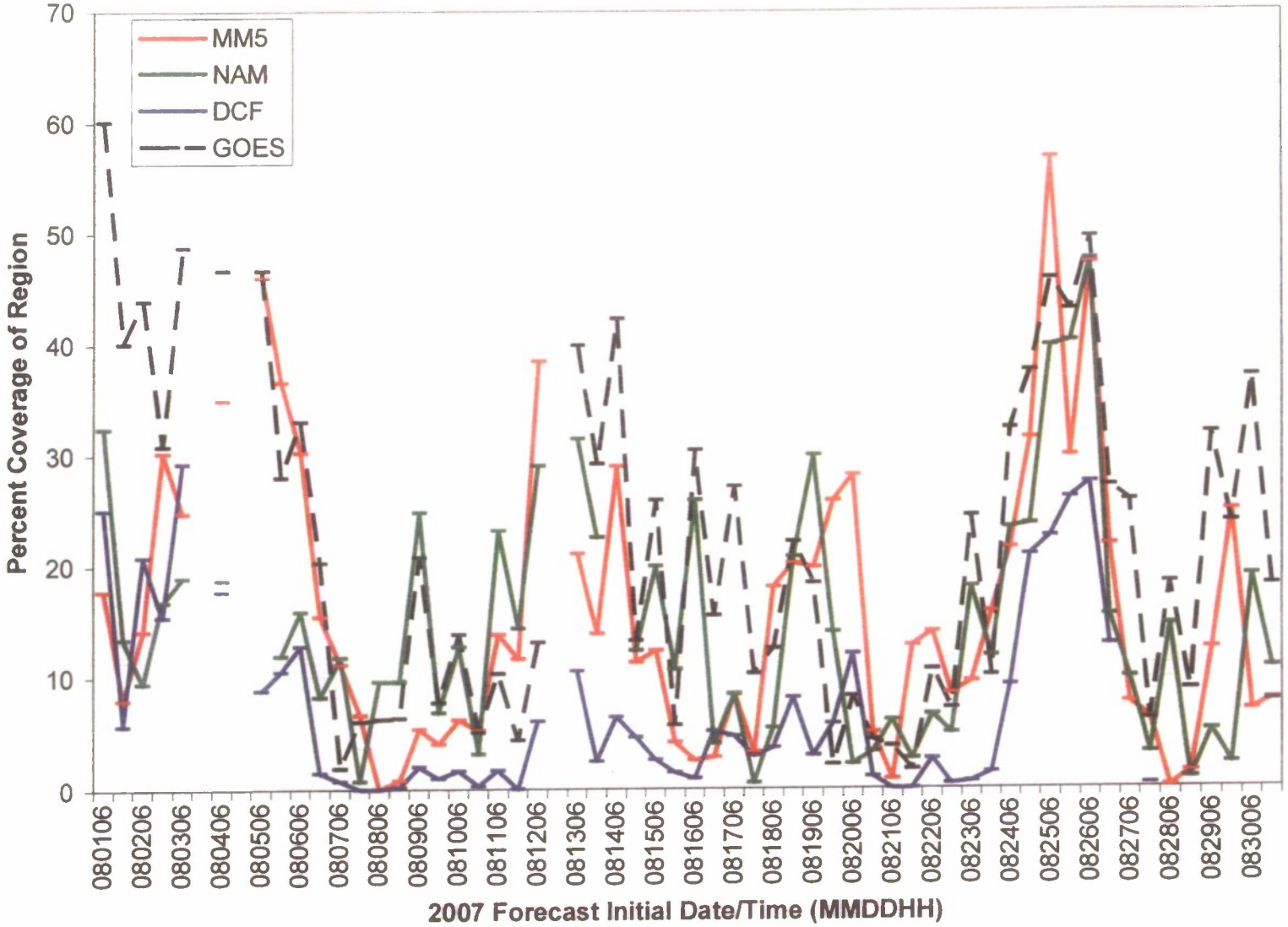

Figure 27. Same as Figure 26 except for SWUS region.

The major value of merit in the individual forecast regional cirrus coverages is the ability to correctly predict the maxima and minima as depicted by the GOES coverages. The models and algorithm show a varying degree of this ability. MM5 and NAM anticipate virtually all of the GOES maxima and minima in both NEUS and SWUS in the Fall period (Figures 20 and 21). However, they exaggerate the coverage in the NEUS maxima but show a varying degree of agreement with GOES in the SWUS. In fact, it appears that MM5 and NAM are able to capture virtually all of the maxima cirrus regional coverages and at the same time realistic portray their durations. Generally there is a tendency by MM5 and NAM to over-predict the maxima in the NEUS and either correctly predict or under-predict in the SWUS. DCF performs considerably better in the NEUS than in the SWUS, but still misses a few maxima in the former region.

4.4 Cirrus Location Forecast Accuracy

To determine the optimum locus of operations in a region, it is important to know in advance where the cirrus clouds will be. Percentages of grid points in which cirrus Y/N presence is correctly and incorrectly predicted by the models/algorithms are presented in contingency tables. Tables 5-8 are the contingency tables for the ice cloud grid point Y/N category percentages in the Fall, Winter, Spring and Summer periods.

Table 5. Fall period contingency table (%) for comparison of grid point cirrus forecasts and GOES within-grid cell cirrus. GOES = Y where ice cloud was detected in at least one within-cell pixel.

		GOES			GOES	
	MM5	Y	N	NAM	Y	N
NEUS/24	Y	32	22	Y	33	15
	N	6	40	N	12	40
NEUS/36	Y	28	20	Y	31	15
	N	9	43	N	14	40
SWUS/24	Y	18	8	Y	19	7
	N	19	55	N	27	47
SWUS/36	Y	17	10	Y	18	6
	N	19	54	N	28	48

Table 6. Same as Table 5 except for Winter period.

		GOES			GOES			GOES	
	MM5	Y	N	NAM	Y	N	DCF	Y	N
NEUS/24	Y	23	17	Y	26	13	Y	11	4
	N	5	55	N	8	53	N	18	67
NEUS/36	Y	21	20	Y	24	14	Y	9	5
	N	6	54	N	9	53	N	19	67
SWUS/24	Y	17	9	Y	16	3	Y	6	1
	N	17	57	N	27	54	N	31	62
SWUS/36	Y	16	9	Y	14	4	Y	4	1
	N	18	57	N	28	54	N	32	63

Table 7. Same as Table 5 except for Spring period.

		GOES			GOES			GOES	
	MM5	Y	N	NAM	Y	N	DCF	Y	N
NEUS/24	Y	28	14	Y	34	8	Y	19	10
	N	14	44	N	16	42	N	22	49
NEUS/36	Y	28	15	Y	32	10	Y	19	10
	N	13	44	N	17	41	N	21	50
SWUS/24	Y	15	11	Y	13	5	Y	1	0
	N	13	61	N	21	61	N	27	72
SWUS/36	Y	15	12	Y	13	6	Y	1	0
	N	13	60	N	21	60	N	27	72

Table 8. Same as Table 5 except for Summer period.

		GOES			GOES			GOES	
	MM5	Y	N	NAM	Y	N	DCF	Y	N
NEUS/24	Y	22	14	Y	27	11	Y	17	10
	N	13	51	N	17	45	N	19	54
NEUS/36	Y	20	14	Y	24	11	Y	16	10
	N	15	51	N	20	45	N	20	54
SWUS/24	Y	9	7	Y	11	4	Y	6	1
	N	21	63	N	26	59	N	24	69
SWUS/36	Y	8	6	Y	10	4	Y	5	1
	N	22	64	N	27	59	N	25	69

In all models/algorithm, regions and forecast durations, the greatest percentage of grid points lie in the N/N category. This means that on average the largest portion of the region is actually and predicted to be cirrus-free. The number just above it (fcst Y / GOES N) indicates the percentage of grid points in which a model/algorithm incorrectly predicts cirrus presence, indicating a falsely predicted cirrus location. These are highest

for MM5 for in the NEUS region. The lower left number in each table (fcst N / GOES Y) represents the percentage of missed cirrus locations by the predictions. Their values are greatest in the SWUS region for all three models/algorithm, especially DCF in the Winter season. The fcst Y / GOES Y are the correctly predicted cirrus grid points, which are consistently more prevalent as a percentage of the region in the NEUS than the SWUS across all seasons and forecast durations.

Tables 9-12 show parameters commonly derived from contingency tables (Wilks, 1995). In this study the hit rate, false alarm rate and bias are used to analyze the cirrus location and spatial extent accuracy. The hit rate is the total percent of grid points where model forecast outcome agreed with the GOES analysis outcome. The results suggest that at any given grid point in a 24-h or 36-h forecast, the cirrus Y/N forecast has at least a 66% chance of being correct. The odds are better in the NEUS for the Winter period and for the SWUS in the Spring. MM5 and NAM hit rate differences vary with season in the NEUS but consistently favor MM5 in the SWUS. DCF forecasts are competitive in hit rate with MM5 and NAM in most seasons/regions except SWUS in Winter and NEUS in the Spring. Hit rate seems to decline slightly with forecast duration.

False alarm rate (FAR) is the percentage of predicted ice grid points that were incorrectly forecasted. High FAR values indicate the tendency to over-predict cirrus occurrence or predictions in areas where cirrus was not detected. Tables 9-12 indicate that MM5 has consistently higher FARs than the NAM in ice cloud prediction. MM5 and NAM FAR values for Fall and Winter are higher in the NEUS region than in the SWUS region but reversed in Spring and in the Summer for MM5. The highest FAR values are

Table 9. Fall period contingency table statistics based on values shown in Table 5. Hit rate = %Y/Y + %N/N, false alarm rate = (% fcst Y/GOES N ÷ % fcst Y) X 100, and bias = % fcst Y ÷ % GOES Y.

Region/Fcst Duration	Model	Hit Rate (%)	False Alarm Rate (%)	Bias
NEUS/24	MM5	72	41	1.42
	NAM	73	31	1.07
NEUS/36	MM5	71	42	1.30
	NAM	71	33	1.02
SWUS/24	MM5	73	31	0.70
	NAM	66	27	0.57
SWUS/36	MM5	71	37	0.75
	NAM	66	25	0.52

Table 10. Winter period contingency table statistics based on Table 6.

Region/Fcst Duration	Model	Hit Rate (%)	False Alarm Rate (%)	Bias
NEUS/24	MM5	78	43	1.43
	NAM	79	33	1.15
	DCF	78	27	0.52
NEUS/36	MM5	75	49	1.52
	NAM	77	37	1.15
	DCF	76	36	0.50
SWUS/24	MM5	74	35	0.76
	NAM	70	16	0.44
	DCF	68	14	0.19
SWUS/36	MM5	73	36	0.74
	NAM	68	22	0.43
	DCF	67	20	0.14

Table 11. Spring period contingency table statistics based on Table 7.

Region/Fcst Duration	Model	Hit Rate (%)	False Alarm Rate (%)	Bias
NEUS/24	MM5	72	33	1.00
	NAM	76	19	0.84
	DCF	68	34	0.71
NEUS/36	MM5	72	35	1.05
	NAM	73	24	0.86
	DCF	69	34	0.73
SWUS/24	MM5	76	42	0.93
	NAM	74	28	0.53
	DCF	73	0	0.04
SWUS/36	MM5	75	44	0.96
	NAM	73	32	0.56
	DCF	73	0	0.04

Table 12. Summer period contingency table statistics based on Table 8.

Region/Fcst Duration	Model	Hit Rate (%)	False Alarm Rate (%)	Bias
NEUS/24	MM5	73	39	1.03
	NAM	72	29	0.86
	DCF	71	37	0.75
NEUS/36	MM5	71	41	0.97
	NAM	69	31	0.80
	DCF	70	38	0.72
SWUS/24	MM5	72	44	0.53
	NAM	70	27	0.41
	DCF	75	14	0.23
SWUS/36	MM5	72	43	0.47
	NAM	69	29	0.38
	DCF	74	17	0.20

due to over-prediction of cirrus during the Fall and Winter periods in the NEUS but the result of mis-location of cirrus predictions in the SWUS in the Spring and Summer. This is reflected in the bias scores. Bias is the ratio of the total percentage of ice grid points predicted to ice grid points detected. Tables 5 and 6 show more predicted than detected ice grid points for the NEUS in Fall and Winter for both MM5 and NAM (greater for MM5), and more detected than predicted for the SWUS (more under-predicted by NAM) in all seasons except MM5 in Spring. Recall that just a single GOES pixel in a grid cell constitutes a GOES ice cloud grid point for the purposes of these statistics. This suggests that in the SWUS the models, especially NAM, misses the frequent scattered, isolated GOES-detected ice cloud (see for example Figure 8). And even though the SWUS FARs are not negligible for either model, the occurrence of fcst Y / GOES N in both models is much smaller in SWUS than in NEUS. DCF has a lower FAR than MM5 or NAM except for during the Spring and Summer in the NEUS region. But it also consistently has the greatest under-prediction bias. Less than ¼ of the actual number of ice grid points are predicted in the SWUS in the Winter, Spring and Summer by DCF.

4.5 Comparison of IWP, CTH and Cirrus Cover

Though the emphasis of this study is to evaluate the predicted location of the cirrus and its coverage, it is also of interest to consider briefly the comparison between predicted and retrieved CTH, IWP and cover. Given the limitations of the GOES retrievals as mentioned in the first paragraph of Section 3 (low CTH bias, low IWP bias), the GOES pixel average within the model/algorithm grid cells can be directly compared with the model/algorithm ice cloud grid point values for all fcst Y / GOES Y grid points. Tables 13 and 14 display the results of this comparison at the Y/Y ice grid points averaged over all forecasts for Winter and Summer. The MM5 IWP averages are 2-3 times larger than the GOES retrieval averages, which is consistent with the suspected low bias of the latter values. NAM IWP averages are consistently an order of magnitude smaller than the MM5 IWP averages, and much smaller than the suspected small GOES values. This is due to the partitioning scheme used in the NAM that assigns less than 10% of the total hydrometeor ice to cloud ice water mixing ratio and over 90% to precipitation ice water mixing ratio (Ferrier, personal communication).

Average CTH are similar for MM5 and NAM in the Winter season. MM5 has somewhat higher CTH averages in the Summer season. Both are higher than GOES in both seasons, consistent with the low bias of the GOES retrievals found by Norquist et al. (2008). This difference decreases when some of the model CTH values are adjusted to the tropopause height. The last column of Tables 13 and 14 indicates that the percentage of ice grid points with CTH that exceed the tropopause height are somewhat greater in the MM5 forecasts than in the NAM predictions. Very few of the GOES CTHs exceed the tropopause height in either season or region.

Table 13. Winter period ice water path (IWP), cloud cover (CC, in parentheses) and cloud top height (CTH) averaged over all forecast Y/GOES Y grid cells (all GOES ice pixels averaged in cell) over all forecasts. Multiple entries for GOES represent comparisons with MM5, NAM and DCF respectively.

Region/Fcst Duration	Model / Analysis	Ave. IWP (g m^{-2}) (Ave. CC, %)	Ave. CTH (km)	Ave. Trop. Adj CTH	% Trop. Adj Pts.
NEUS/24	MM5	60	10.3	9.7	68
	NAM	6	10.0	9.6	53
	GOES	23, 22 (88)	9.0, 8.9, 9.4	9.0, 8.9, 9.4	6, 2, 6
	DCF	(52)	13.3	10.5	100
NEUS/36	MM5	54	10.0	9.6	59
	NAM	6	9.9	9.6	52
	GOES	23, 22 (85)	8.9, 8.8, 9.3	8.9, 8.8, 9.3	7, 2, 7
	DCF	(58)	13.5	10.4	100
SWUS/24	MM5	41	10.1	9.8	39
	NAM	3	10.1	9.8	34
	GOES	19, 18 (90)	9.4, 9.3, 9.6	9.3, 9.3, 9.6	7, 5, 4
	DCF	(79)	13.5	10.9	95
SWUS/36	MM5	38	10.2	9.9	39
	NAM	3	10.2	9.9	35
	GOES	18, 18 (88)	9.4, 9.4, 9.5	9.4, 9.3, 9.5	5, 5, 3
	DCF	(76)	13.7	10.9	97

Table 14. Same as Table 13 except for Summer period.

Region/Fcst Duration	Model / Analysis	Ave. IWP (g m^{-2}) (Ave. CC, %)	Ave. CTH (km)	Ave. Trop. Adj CTH	% Trop. Adj Pts.
NEUS/24	MM5	28	11.4	11.3	20
	NAM	3	11.0	10.9	17
	GOES	21, 19 (81)	10.7, 10.5, 10.6	10.6, 10.5, 10.6	2, 4, 2
	DCF	(65)	15.3	13.5	67
NEUS/36	MM5	27	11.6	11.5	22
	NAM	3	11.2	11.1	22
	GOES	21, 20 (80)	10.7, 10.6, 10.6	10.6, 10.5, 10.5	3, 3, 3
	DCF	(62)	15.0	13.5	63
SWUS/24	MM5	24	12.2	12.1	10
	NAM	3	11.0	10.9	3
	GOES	20, 19 (88)	11.1, 11.0, 11.2	11.1, 11.0, 11.1	0, 1, 0
	DCF	(67)	13.4	13.1	14
SWUS/36	MM5	23	11.9	11.9	8
	NAM	3	11.0	11.0	2
	GOES	20, 20 (85)	11.0, 11.0, 11.1	11.0, 11.0, 11.1	0, 0, 1
	DCF	(63)	13.3	13.0	15

DCF cloud top height comparisons with co-located GOES retrievals reveal that

the former are on average from 2 to 4 km higher. This suggests that the DCF CTH values are probably too high, especially in the NEUS in both seasons and in the SWUS in the Winter. This is reflected in more than 95% of the Y/Y DCF CTH values exceeding the tropopause heights. Grid cell cirrus cover for compared DCF and GOES Y/Y grid points reveals a 15-30% under-prediction. This is due in large part to the categorical nature of the DCF cloud cover diagnosis, which restricts cloud amounts to no more than 90% coverage even in the midst of large cirrus masses (see Figure 7). The great majority of GOES grid cell coverages are overcast in such environments.

Seasonal period averages of IWP, CTH and cirrus cover do not reveal the nature of the predictions in comparison with GOES. Some insight on this can be gained by examining the frequency distribution of the predicted and analyzed values of these cirrus properties. This was done only for the fcst Y / GOES Y points in order to allow a fair comparison between the predicted and detected values. Figure 28-33 show frequency distribution plots for the NEUS region only for Winter and Summer periods, since fcst Y / GOES Y counts in the SWUS were considerably lower.

Frequency distribution of CTH in Figures 28, 29, 31 and 32 make it clear that most of the predicted CTH values are larger than the GOES algorithm-retrieved CTH at the comparison grid points. For MM5 and NAM these are concentrated at 1-3 height categories larger than the GOES peak category, while for DCF there are multiple maxima in the frequency distribution. Again, this is due to the categorical predictands in the DCF method that result in specific CTH assignments. The cloud cover distribution for DCF and GOES shown in Figures 29 and 32 reinforce the point made earlier that the majority of grid cells were analyzed as overcast with cirrus, whereas the highest cirrus

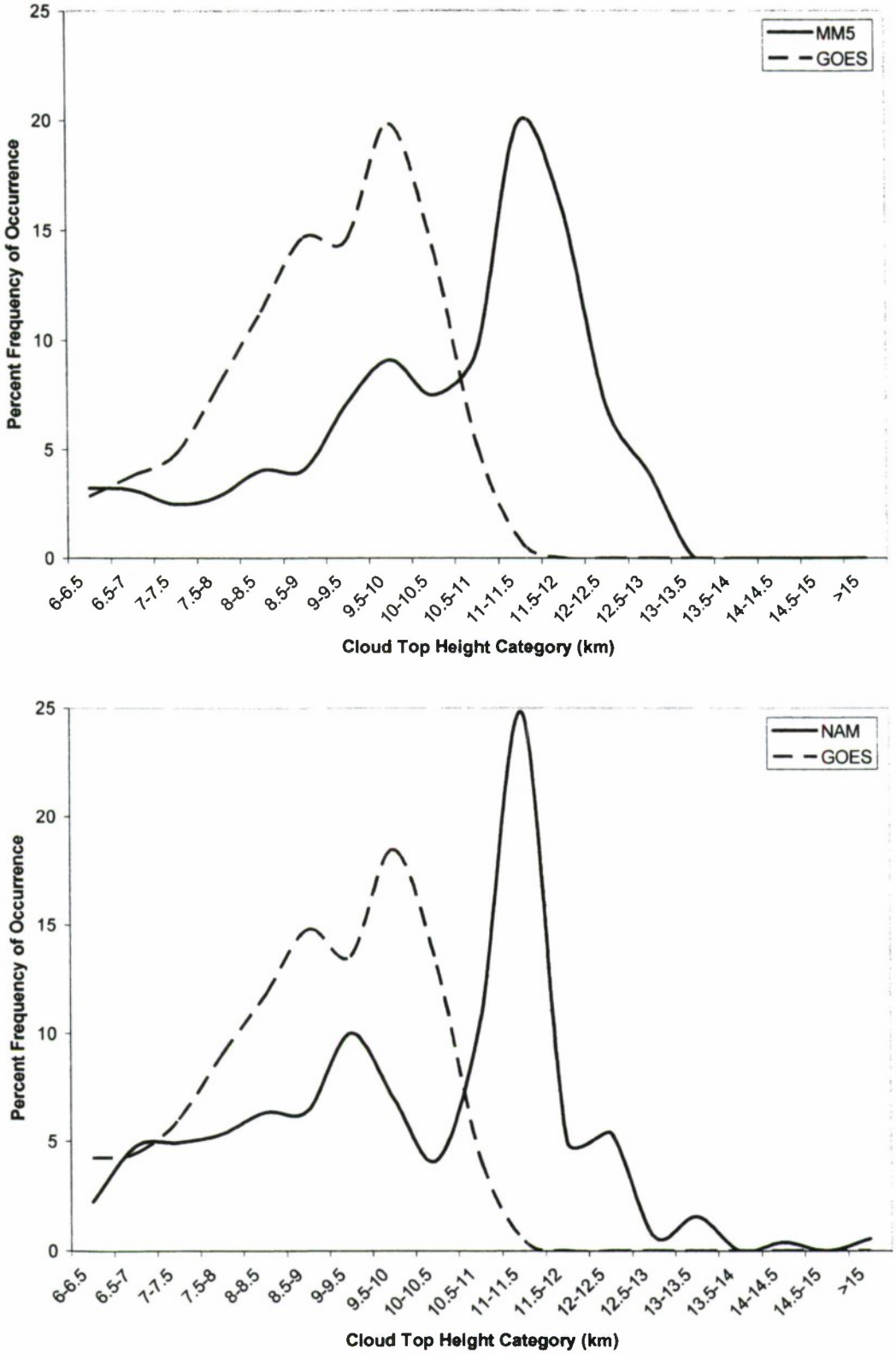

Figure 28. NEUS region cloud top height category frequency distribution for all forecast Y / GOES Y grid cells for the Winter period from 24-h (top) MM5 and (bottom) NAM ice cloud forecasts and GOES pixel retrievals averaged within the grid cells.

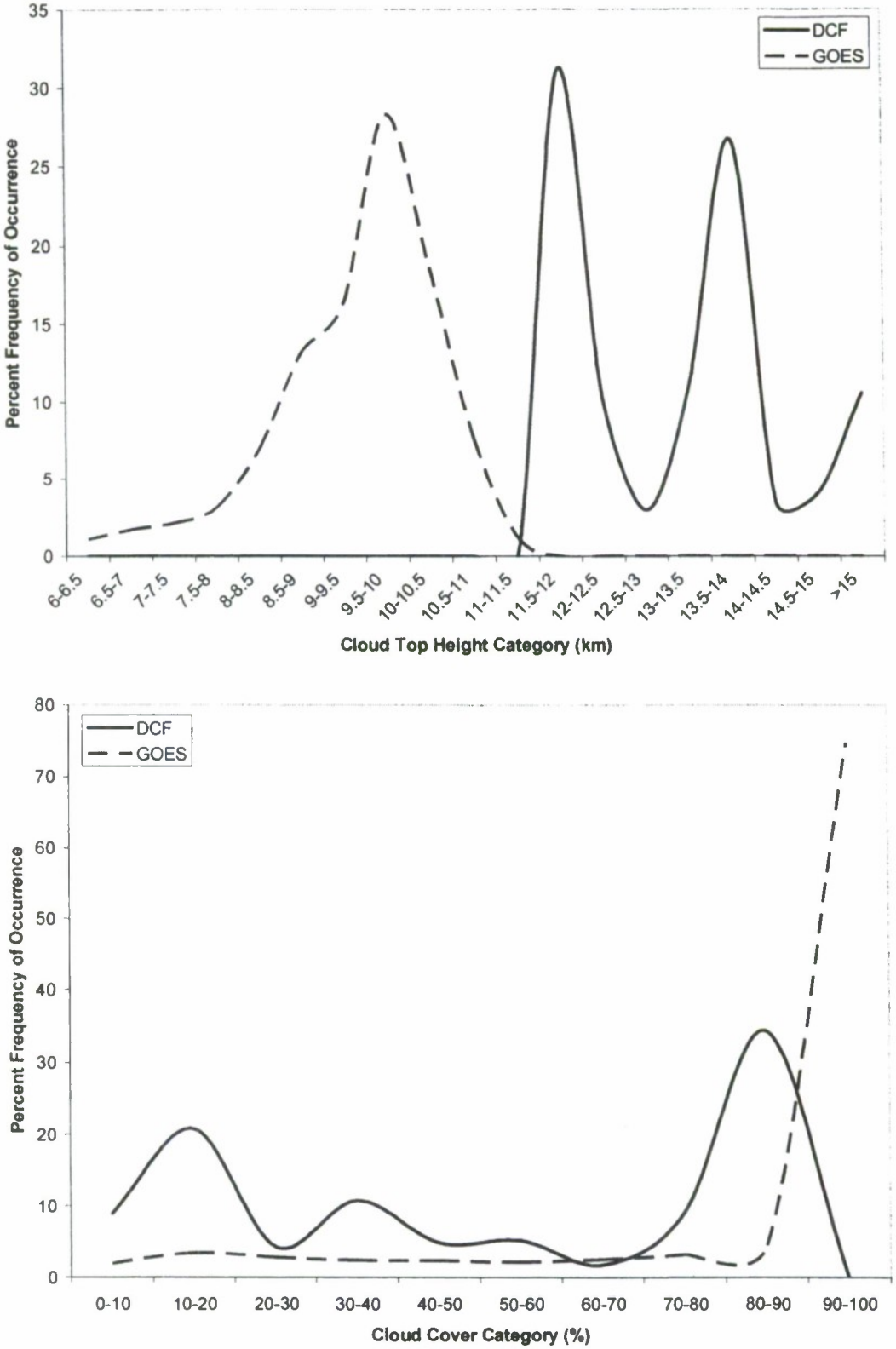

Figure 29. Frequency distribution of (top) cloud top height and (bottom) cirrus cover category for all DCF forecast Y / GOES Y grid cells for the Winter period in the NEUS region.

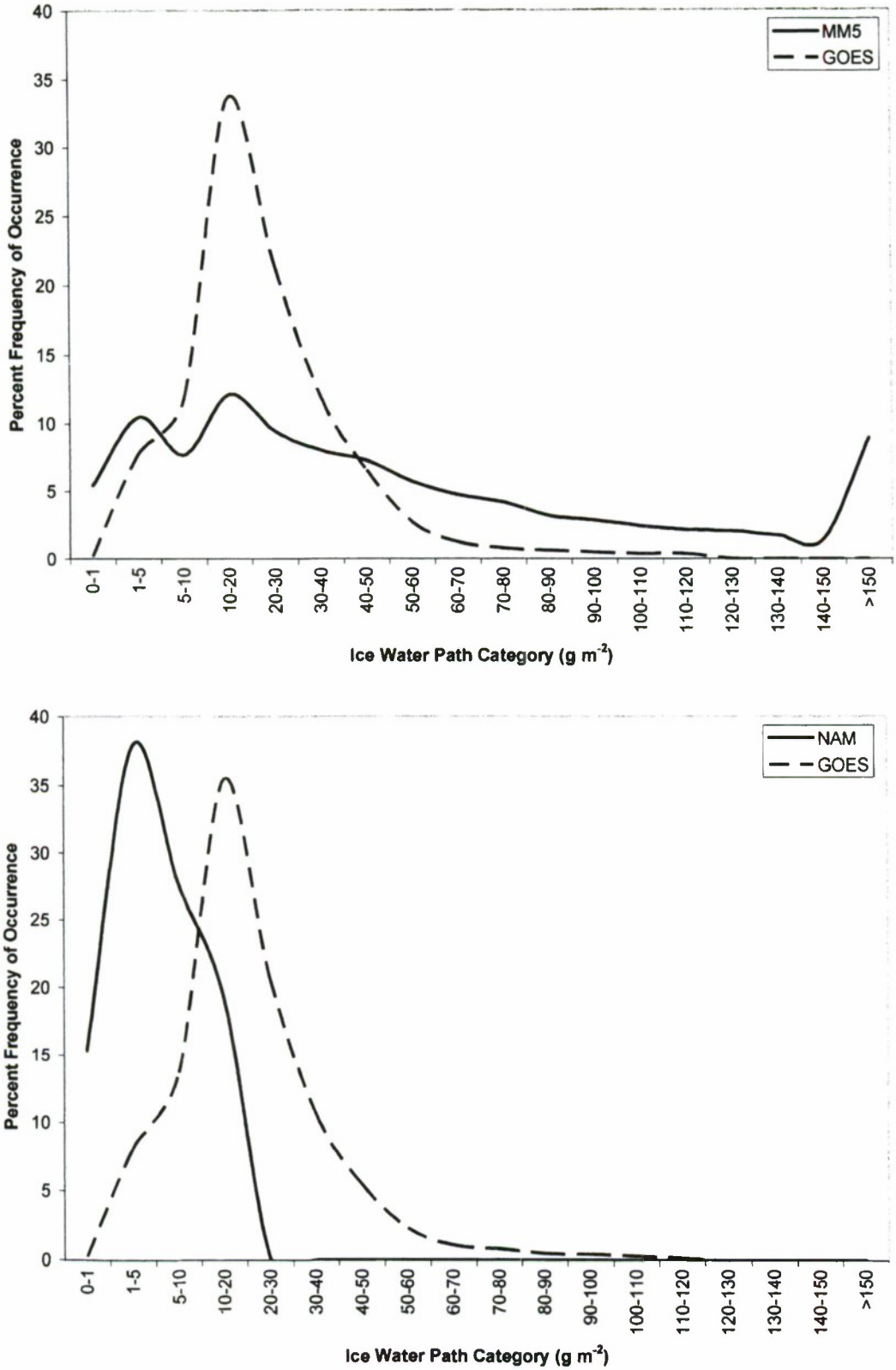

Figure 30. Same as Figure 28 except ice water path category.frequency distribution for (top) MM5 and (bottom) NAM forecasts.

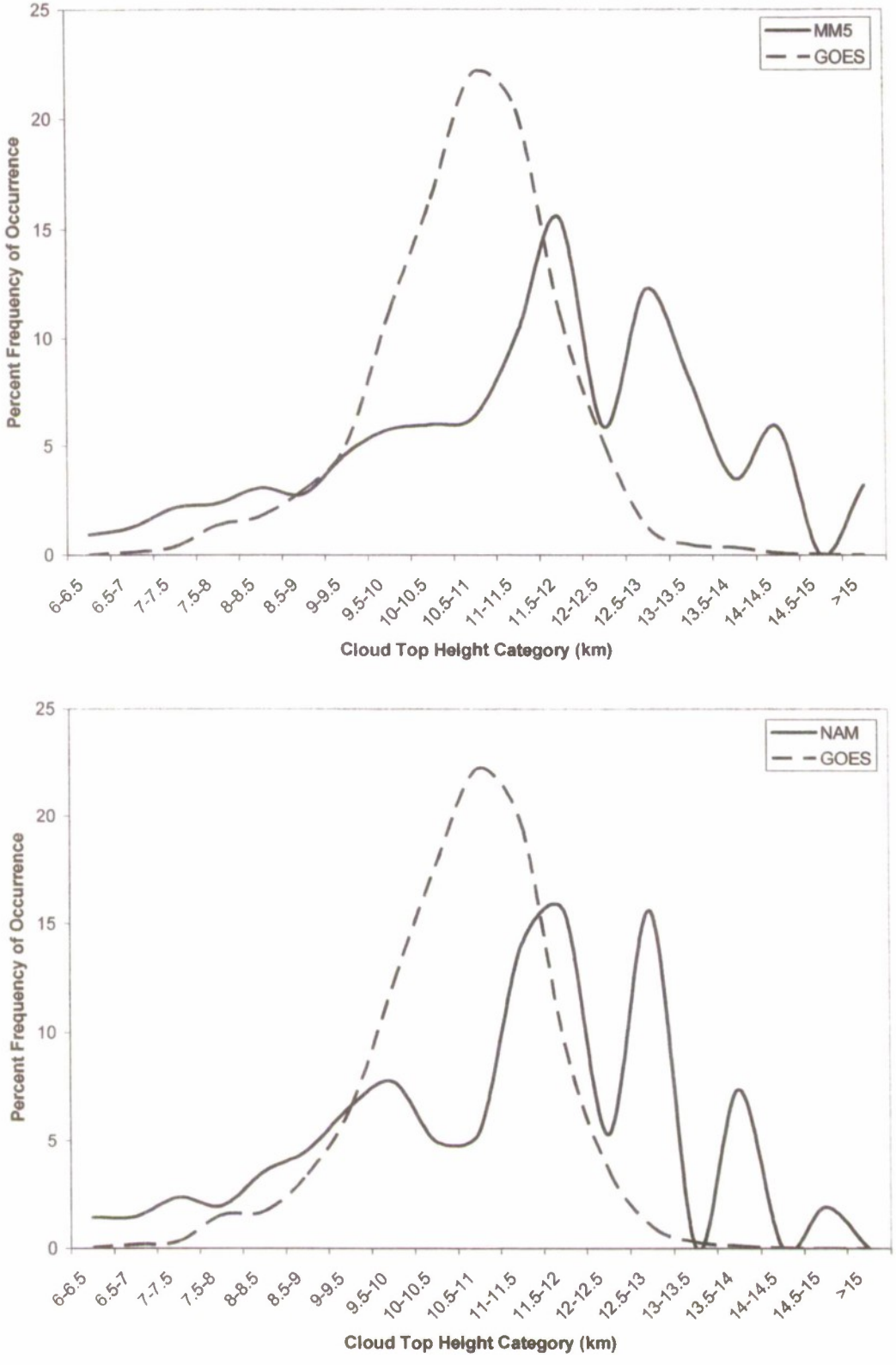

Figure 31. NEUS region cloud top height category frequency distribution for all forecast Y / GOES Y grid cells for the Summer period from 24-h (top) MM5 and (bottom) NAM ice cloud forecasts and GOES pixel retrievals averaged within the grid cells.

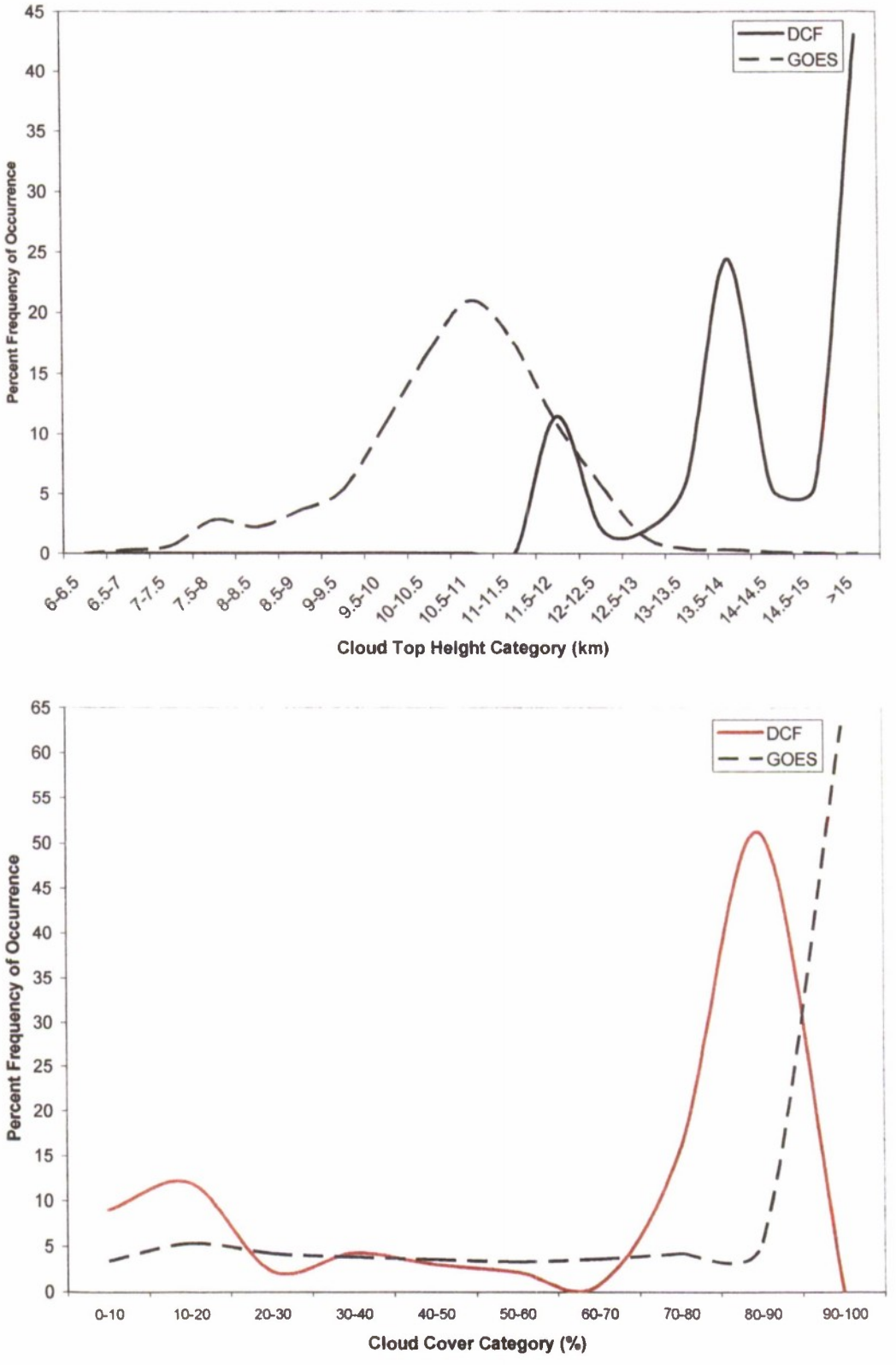

Figure 32. Frequency distribution of (top) cloud top height and (bottom) cirrus cover category for all DCF forecast Y / GOES Y grid cells for the Summer period in the NEUS region.

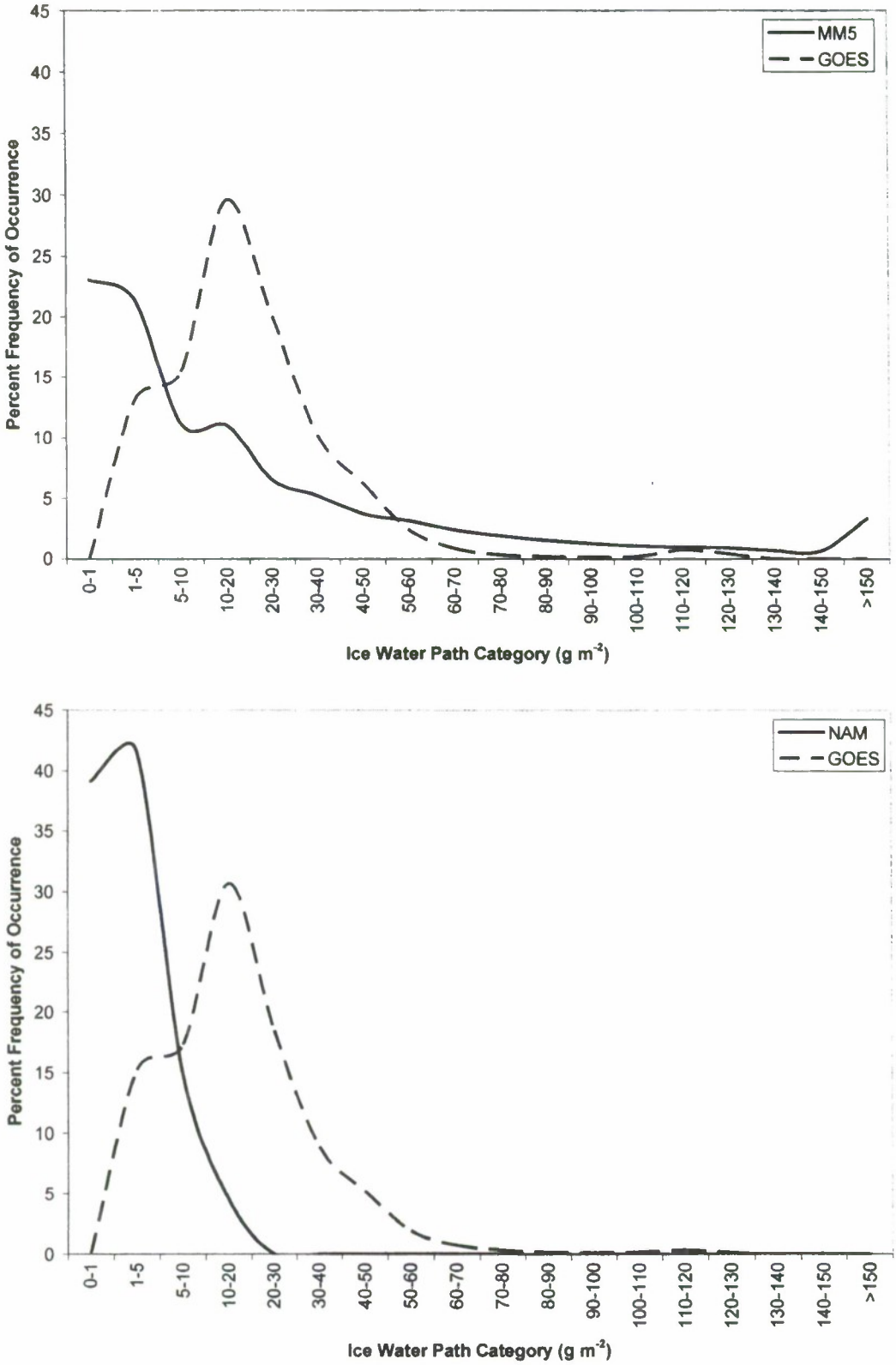

Figure 33. Same as Figure 31 except ice water path category.frequency distribution for (top) MM5 and (bottom) NAM forecasts.

cover category in the categorical DCF diagnosis is in the 80-90% range. Even so, there are a non-negligible number of DCF ice cloud grid cells at the comparison points that have much lower (10-20% and 30-40%) cover category values.

IWP frequency distributions based on fcst Y / GOES Y grid cells are shown in Figures 30 and 33. MM5 predictions are spread across the entire range of IWP categories, whereas NAM forecasts are concentrated mainly in the categories less than 10 g m^{-2}. The peak category for the NAM IWP values is less than that of GOES and more concentrated in numbers of categories. MM5 actually shows a minor maxima at the highest IWP category, as indicated in the MM5 map plot as shown in Figure 6.

5 SUMMARY OF CIRRUS PREDICTION PERFORMANCE

Based on the results presented in this paper, the following summary of the characteristics of each of the three cirrus forecast techniques is presented. This summary can guide the use of the MM5, NAM and DCF cirrus forecasts in support of military system deployment in the two regions studied in this project.

Major Study Findings, Fall Period

- NEUS
  - MM5, NAM over-predict cirrus coverage
  - MM5, NAM cirrus event timing is good
  - Grid cell comparisons – model vs. GOES
    - Hit Rate comparable for MM5, NAM
    - False Alarm rate better for NAM than MM5
    - Bias – MM5: large +, NAM: small +
- SWUS
  - Cirrus coverage: MM5 good, NAM small –
  - MM5, NAM cirrus event timing is moderate
  - GRID cell comparisons – model vs. GOES
    - Hit Rate better for MM5 than NAM
    - False Alarm rate slightly better for NAM than MM5
    - Bias – MM5: moderate –, NAM: large –

Major Study Findings, Winter Period

- NEUS
  - MM5, NAM over-predict cirrus coverage, DCF under-predicts
  - MM5, NAM cirrus event timing is good, DCF is moderate
  - Grid cell comparisons – model/algorithm vs. GOES
    - Hit Rate comparable for MM5, NAM, DCF
    - False Alarm Rate worst for MM5, best for DCF
    - Bias – MM5: large + ; NAM: small + ; DCF: large –
- SWUS
  - Cirrus coverage: MM5 good, NAM small – , DCF large –
  - MM5, NAM cirrus event timing is moderate, DCF is fair
  - Grid cell comparisons – model/algorithm vs. GOES
    - Hit Rate best for MM5; NAM and DCF are comparable
    - False Alarm Rate worst for MM5, best for DCF
    - Bias – MM5: small – ; NAM: large – ; DCF: huge –

Major Study Findings, Spring Period

- NEUS
  - MM5, NAM over-predict cirrus coverage, DCF slightly under-predicts
  - Good cirrus event timing for MM5, NAM, DCF is fair
  - Grid cell comparisons – model/algorithm vs. GOES
    - Hit Rate best for NAM, worst for DCF
    - False Alarm Rate best for NAM, comparable for MM5, DCF
    - Bias – MM5: about right ; NAM: small – ; DCF: moderate –
- SWUS
  - Coverage: MM5 over-predicts, NAM slightly under-predicts, DCF ~ 0
  - MM5 and NAM cirrus event timing is good, DCF virtually no cirrus
  - Grid cell comparisons – model/algorithm vs. GOES
    - Hit Rate best for MM5, comparable for NAM, DCF
    - False Alarm Rate better for NAM than MM5, DCF ~ 0
    - Bias – MM5: about right; NAM: large –, DCF: extreme –

Major Study Findings, Summer Period

- NEUS
  - MM5, NAM over-predict cirrus coverage, DCF about right
  - MM5, NAM and DCF cirrus event timing is good
  - Grid cell comparisons – model/algorithm vs. GOES
    - Hit Rate comparable for MM5, NAM, DCF
    - False Alarm Rate worst for MM5, best for NAM
    - Bias – MM5: about right ; NAM: small – ; DCF: large –
- SWUS
  - Cirrus coverage: MM5, NAM moderately low, DCF extremely low
  - MM5, NAM cirrus event timing is moderate, DCF is fair
  - Grid cell comparisons – model/algorithm vs. GOES
    - Hit Rate best for DCF, worst for NAM
    - False Alarm Rate worst for MM5, best for DCF
    - Bias – MM5: large – ; NAM: large – ; DCF: huge –

Overall Conclusions

- NAM probably the best performer in NEUS, MM5 likely best in SWUS
- DCF suffers from under-prediction, especially in SWUS
- MM5, NAM could be useful for next-day regional coverage guidance
- DCF would benefit from regional statistical relationship development
- DCF cirrus top heights should be reduced
- There is a lot of room for improvement in operational cirrus prediction.